2016

Numerical Simulation of Continuous Rotary Extrusion of Magnesium AZ91 Alloy

Nijenthan Rajendran
Lehigh University

Numerical Simulation of Continuous Rotary Extrusion of Magnesium AZ91 Alloy

by

Nijenthan Rajendran

A Thesis

Presented to the Graduate and Research Committee

of Lehigh University

in Candidacy for the Degree of

Master of Science

Lehigh University

May 2016

This thesis is accepted and approved in partial fulfillment of the requirements for the Master of Science.

_____

Date

_____

Wojciech Z. Misiolek

Thesis Advisor

_____

D. Gary Harlow

Department Chair Mechanical Engineering and Mechanics

ACKNOWLEDGEMENTS

I would like thank my advisor Professor Wojciech Z. Misiolek, without whom this work might not have been possible. Thanks for separating time for me even with your tight schedule. I am also in a great debts to Professor Henry S. Valberg from Norwegian University of Science and Technology. Most of my numerical simulation work has been done under his guidance. Thank you sir for the help and motivation that you offered. I learned a lot from your guidance.

I also wanted to thank Mrs. Monika Mitka Institute for Non-ferrous Metal in Skawina, Poland and MelTech equipment manufacturer in UK for sharing information with me, and helping me improving my work.

I would like to extend my gratitude to all Institute for Metal Forming member for helping me in my work. Especially Ahmad Chamanfar and John Plumeri answering any of my question without getting mad, even though sometimes I make you guys mad. I would also like to thank both mechanical and materials department coordinators JoAnn Casciano, Janie Carlin and Lisa Arechiga for their help.

I also wanted to thank my friends, roommates who kept on encouraging me. And finally I wanted to thank my parents M. Rajendran PhD., and R. A. Sasikala MA., for giving me this opportunity and believing in me.

TABLE OF CONTENTS

LIST OF FIGURES

LIST OF TABLES

ABSTRACT

Continuous Rotary Extrusion (CRE) is well known process known also under Conform name used for extrusion of Aluminum and Copper alloys. Magnesium is the lightest major engineering construction metal, and due to its good mechanical properties, it has been used increasingly as a substitute for aluminum and steel in particularly aerospace and automotive industries. Magnesium alloys are difficult to deform at room temperature due to its hexagonal crystal structure. Therefore, Magnesium has to be processed at elevated temperature in order to take advantage of the increased ductility at these temperatures. From the literature survey it is clear that better mechanical properties of Magnesium alloys can be achieved by both hot deformation and dynamic recrystallization and CRE could improve Magnesium alloys properties as it is capable of refining and improve the grain structure. In this work an investigation has been carried out to study the mechanics of the CRE process when used for Magnesium alloys AZ91, by means of FEM- modelling. Using FEM-modelling of the CRE process, mapping of the nature of metal flow by means of temperature, strain and strain rate distribution in deformed material was performed. This allowed different process parameters that are required for the process quality to be analyzed. Four different numerical models of Continuous Rotary Extrusion for Magnesium AZ91 alloy were developed using DEFORM-3D^{TM} software and the influence of different process parameters on the extrudate quality was studied. Through the numerical analysis investigation of the influence of the effective stress, strain, temperature, strain rate and velocity in the CRE process on outcome of four different models was studied. The material behavior under different processing condition has been compared. Process condition which causes plugging and other defects are discussed. The work has been successful as the FEM- model was able to represent the mechanics of the Magnesium alloy processed by the CRE process.

1 INTRODUCTION

1.1 Magnesium and magnesium alloys

In World War I and II Magnesium was used in nuclear industry, military aircraft, and the most significant application was its first automotive industrial application in the VW beetle, but after that the use of Magnesium was reduced. In 1944 the consumption had reached 228,000 ton but was reduced after the war to 10,000 ton per annum. [1] The important problem in the growing automobile industry is environmental pollution caused by the emission from the automobiles. To solve this problem many solutions were proposed like changing aerodynamic shape, increasing the efficiencies of engines or producing hybrid vehicles as well as reducing the weight of the vehicle. It has been found that more than 50% of the fuel consumption is mass dependent, hence reducing the weight will have huge impact on pollution. To attain this reduction in weight, the automobile industry considered aluminum, titanium, but Magnesium is the most attractive choice as it is the lightest material among them. In 1998 with this renewed interest Magnesium consumption has climbed to 360,000 tons per annum at a price of US$3.6 per kg. The growth rate over the next 10 years has been forecast to be 7% per annum. At present American companies like General Motors, Ford, Fiat and Chrysler are considering use of Magnesium. However, still its use is a small fraction when compared to aluminum, which has reached up to 123 kg per vehicle. [1]

While Magnesium is the lightest major engineering construction metal and with a density of 1.74 g/cm^3 it is 35% lighter than aluminum (2.70 g/cm3), and 78% lighter than steel (7.85 g/cm3). Moreover, it has some ductility, good recyclability, and improved vibration and noise characteristics as compared to other structurally used metals. In addition to that it is also tougher than plastics and its electromagnetic interference (EMI) shielding and heat dissipation values are also much higher. This is why Magnesium was called as “the 21th century’s engineering material”.

Some of the well-known series in this category are AZ, ZK, WE and ZE as shown in Table 1. To improve the characteristics of pure Magnesium several alloying elements are used, like in the AZ series aluminum and zinc are added to strengthen the workability of these alloys. Similarly in the ZE series rare earth elements like cerium, yttrium and neodymium are added along with zinc to increase the ductility as well as the material electromagnetic interference (EMI) shielding and heat dissipation values. The main problems are with Magnesium are difficulty to deform it, due to its hexagonal closed pack (hcp) crystal structure and few slip systems, is less ductile at room temperature and problem of corrosion resistance has not been solved. The problem of limited ductility is overcome by forming Magnesium at elevated temperature. [2] [3]

Table 1. Nominal Composition. [4]

	Alloying elements Composition (%)					
Magnesium alloys	Al	Mn	Zn	Zr	RE	Y
AZ	1.2-9	0.10-0.13	0.4-2			
ZK			2.3-6	0.45-0.7		
WE				0.7	3-3.4	4-5.2
ZE			4.2-5.8	0.7	1.2-2.6	

Presently the Magnesium alloys are mainly processed by die casting or thixo-forming processes. However, the die cast Magnesium product have disadvantages such as pin holes, porosity, cold shuts and low mechanical properties. Although semisolid methods such as thixomolding or rheomolding, can reduce the scarping rate of casting, the high temperature causes die erosion which is still needed to be solved for industrial practice. Processing magnesium by forming is the best way as it offers fine-grained microstructure without porosity [5]

1.1.1 Alloy Development

The material properties demanded by the automobile industry and other large scale users of structural materials, have stimulated the development of Magnesium alloys. It is impossible to obtain all the desired mechanical properties with a single alloying element. Figure 1 shows the different trends in alloy development depending on the main requirement. [1]

1.1.2 Specific Strength

Magnesium alloy AZ91 covers major application of magnesium. Even though only 6% of Al is used it forms the basic alloying element, it provides good combination of strength and ductility. Figure 1 Shows that the Mg-Al alloy can be developed further for die-casting by adding Manganese Mg-Al-Mn, by adding zinc for wrought alloys Mg-Al-Zn and for sand casting by adding silicon Mg–Si, Mg–Al–Ca–(RE) rare earth elements. Addition of Li decreases strength but increases ductility, but the strength can be improved through age hardening. Due to its high specific strength there are numerous applications of Magnesium alloys such as automobile constructional parts, components and machine tool parts. [1]

1.1.3 Ductility

There are many technological processes which demand the material with high ductility. Ductility of a material is determined by the number of active slip system. Magnesium due to its hcp structure, has only two slip systems basal and secondary present at room temperature. This limits the ductility of Magnesium at room temperature. At elevated temperature additional pyramidal system comes into play. This behavior can be influenced by alloying, but as long as the structure remains hexagonal the effect is limited. A mixture of two phases bcc and hcp in magnesium by developing alloys based on Mg–Si and Mg–Al–Ca–(RE) and Mg–Li–X can

improve the material ductility. In addition to this ductility can be improved by formation of fine grains and texture control. [1]

1.1.4 Fiber and particle reinforced magnesium

The use of fiber and/or particle reinforcement is needed to get desired properties which cannot be achieved through conventional alloying practice. Al_2O_3, SiC or carbon are the usual reinforcement material. Fiber reinforcement are usually added to metal matrix to improve elastic modulus, wear and creep resistance. The major problem in fiber reinforcement is that chemical reactivity of magnesium with the reinforcement, which might weaken the reinforcement material. The major task in this process is finding a proper matrix element and proper fabrication process. [1]

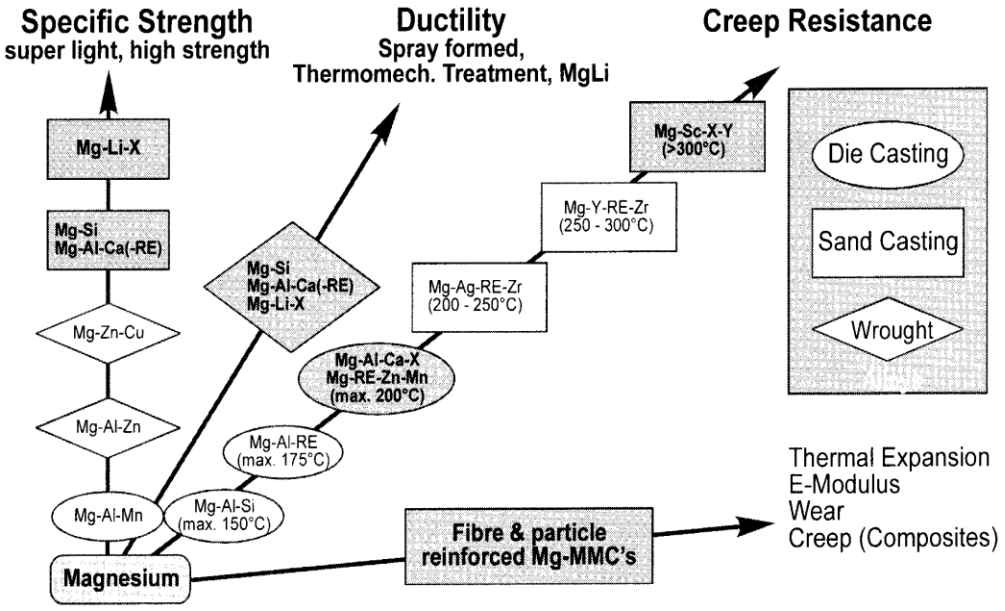

Figure 1. Direction of alloy and metal matrix composite development. [1]

Mabuchi M et al, have recycled machined chips of AZ91 magnesium alloy by extrusion process and compared extrudates with those of sintered compact, and cast material processed from of the same material machined chips. They found extrudates processed from machined chips

showed higher strength at room temperature. They also found that machined chip processed by extrusion at 300 and 400° C showed superplastic behavior at 300° C. Based on their observations they made a conclusion that hot extrusion is an effective way to processes the magnesium machined chips. [6]

Watanabe H et al, in their work found out that in hot extrusion of AZ91 metal ingot at relatively low temperature of 300° C with a reduction ratio of 44, a very fine grain size of 1.7 micro meters was obtained. They concluded that by lowering the temperature, we can obtain finer grain size. They also found that at higher strain rate, higher than 10^{-2} sec^{-1} superplasticity was attained for the same process at ~275° C, however a superplastic behavior disappeared above 325°C because of rapid grain growth. [7]

Ravi Kumar N.V et al, in their work found out that very fine microstructure with average grain structure of 5 micro meters can by produced by dynamic recrystallization during high temperature extrusion of AZ91 alloy.[8]

Liu G et al, in there study of metal flow and weld seam formation in porthole die during extrusion of magnesium AZ31 alloy that the distinctive stages of the extrusion welding is affected by the extrusion pressure. They also found that weld seam had a poor mechanical quality due to air entrapment. They also saw that as ram speed increased the bonding at the longitudinal weld seams increased. [9]

Form these studies it is clear that to improve mechanical properties of the magnesium alloy we need to a fine grain structure is desired, which can be achieved by a process which has both hot deformation and dynamic recrystallization (DRX), and it seems extrusion is the effective way to process the magnesium alloy as it results in fine grain structure increasing the strength and ductility.

1.2 Extrusion Processes

Extrusion is a process by which a billet is reduces in cross section by pushing it through the die orifice. In general, the extrusion process is used to produce cylindrical or hallow parts, however it is also capable of making intricate and complex shapes form easily extrudable metals, such as aluminum and copper. Extrusion is generally a hot forming process, but cold extrusion is also possible for many metals and becoming more commercially important process. Extrusion is listed under the "compressive deformation" in the classification of deformation processes given in German standards DIN 8582 and 8583. As shown in Figure 2 all the principal stress those acts in extrusion are compressive in nature, in contrast to most of the other deformation processes. This allows reaching high strain without fracture. The workability increase with increase in mean stress or decreasing relative mean stress value, in case of extrusion the relative mean pressure value is low ($\sigma_1 > \sigma_2 > \sigma_3$, $\sigma_m = ((\sigma_1 + \sigma_2 + \sigma_3)/3)$). Hence the workability in extrusion is higher for given material, this is the reason most of the metal which are difficult to form are deformed using extrusion process. [10] [12] The Classification of the extrusion processes shown in the Figure 3. [11]

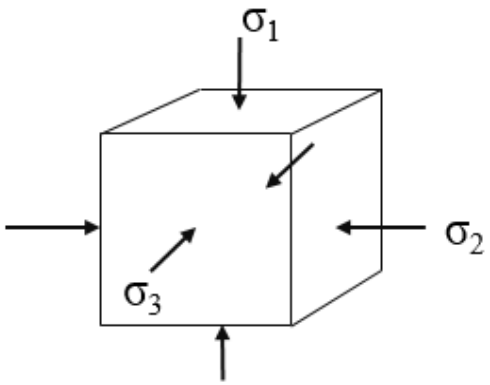

Figure 2. Variation of axial stress for extrusion.

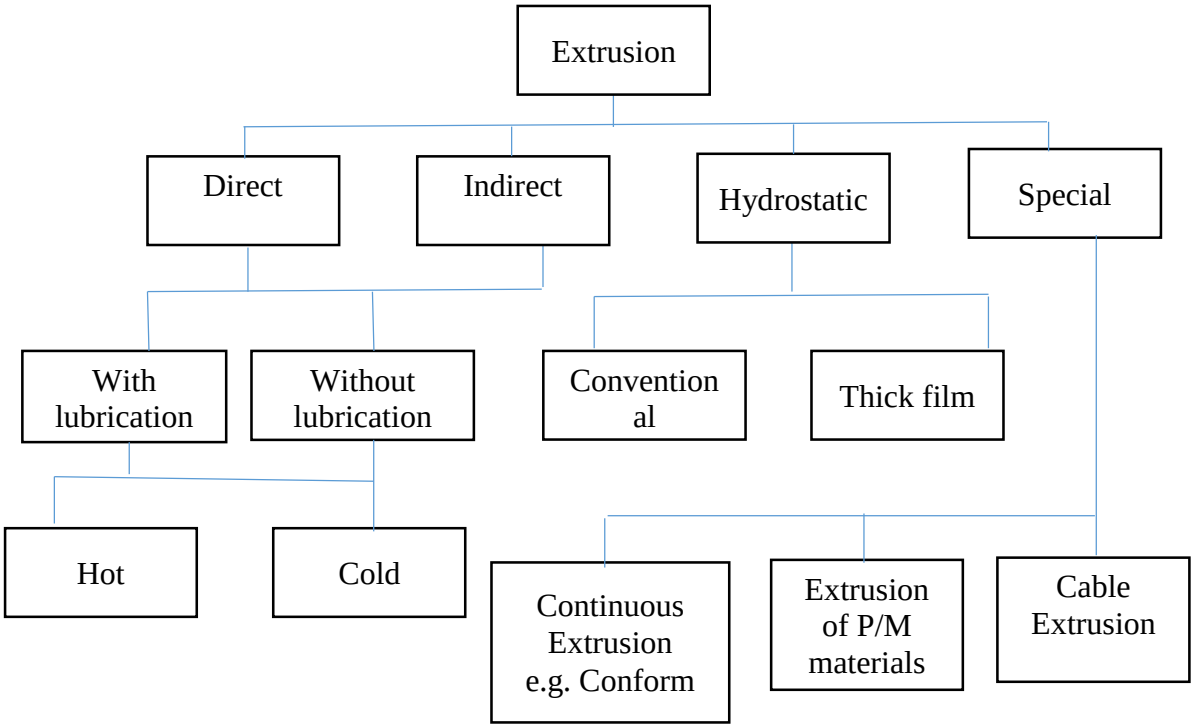

Figure 3. Classification of Extrusion processes. [11]

1.2.1 Direct Extrusion

Direct extrusion shown in Figure 4 is the most frequently used extrusion process. In direct extrusion the billet placed inside the container is pushed through the die orifice by a ram. Because the billet is forced with high pressure billet material tends to pressure-weld on the ram head [12]. To avoid this, a dummy block or pressure pad is placed at the end of the ram in contact with the billet. Direct extrusion can be divided into 4 groups according to the billet temperature and also the use of lubrication. If the billet is heated above the recrystallization temperature before it is placed inside the container then it is known as hot extrusion. Hot working is a standard in the extrusion practice. Cold extrusion is a special process; here the billet is loaded into the container at room temperature without heating. Cold extrusion has several advantages over hot extrusion such as, oxidation free, higher mechanical properties, close geometrical tolerances, better surface

finish, and faster extrusion speeds with alloys susceptible to hot shortness. The limiting factor in cold extrusion is stresses in the tooling, the maximum stem pressure that can applied is 1400N/mm^2. Lubrications is used mainly for extrusion of alloy steels, titanium and copper as there will be lot of friction between the billet material and the tooling. To reduce the extrusion load and to increase the extrusion speed, there will be a thin layer of lubricant used between the billet material and the tooling. Aluminum and aluminum alloys are usually extruded without lubrication. In the extrusion process the surface of the billet material will try to flows towards the center, which might cause extrusion defects. To avoid this extrusion of aluminum is done without lubrication, however to remove the dummy block at the end of the extrusion process the rear end of the billet is lightly lubricated. [10] [12]

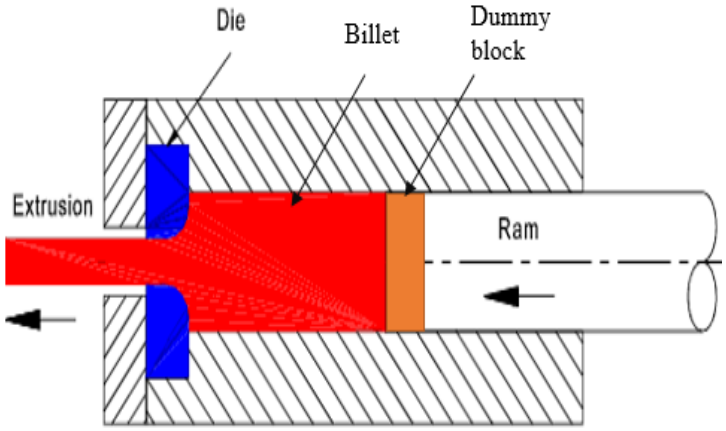

Figure 4. Direct Extrusion.

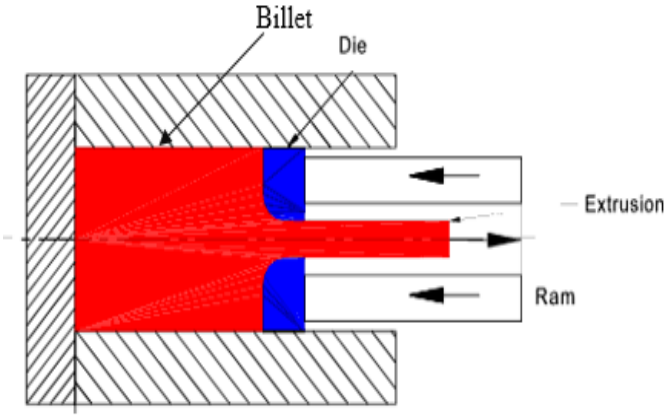

Figure 5. Indirect Extrusion.

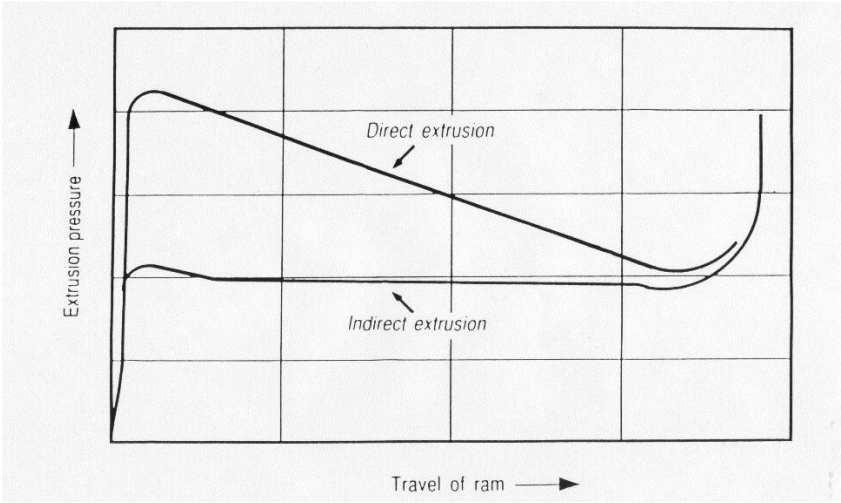

Figure 6. Extrusion pressure graph.

1.2.2 Indirect Extrusion

Indirect extrusion shown in Figure 5 is less commonly used. In indirect extrusion the billet is placed inside the container, one end of the container is blocked with a closing pad with the billet stacked against it, from the other end a die placed in front of the hollow ram is pushed against the billet and as the billet will be extruded through the die and the hollow ram. This process is called

indirect extrusion, because of the direction of metal flow is opposite to that of the ram direction of movement.

Indirect extrusion has certain advantages over direct extrusion, since the billet is kept stationary in indirect extrusion, less extrusion force is required as shown in Figure 6 and in addition there is a better dimensional stability of the extruded product. However direct extrusion is most commonly used because of two facts, one is that in indirect extrusion the extruded parts must be taken out through the hollow ram, and it is difficult to design a hollow ram strong enough to withstand the high extrusion load. The second one is the surface quality of the extruded product is inferior. Billets produced in continuous casting process have the limited quality of the billet surface, hence most of the billet have to be machined before indirect extrusion. [10] [12]

1.2.3 Hydrostatic extrusion

In hydrostatic extrusion shown in Figure 7 the billet is placed inside the pressurized hydrostatic medium in the sealed container. The billet must be sealed against the die when hydrostatic medium is compressed to the working pressure to ensure that it reaches the extrusion pressure. The liquid medium is pressurized and in turn it pressurize the billet and push it through the die. Main advantage of hydrostatic pressure is that as the billet does not touch the container wall during extrusion there is only friction between the fluid and billet surface which is negligible when compared to the forces in hydrostatic extrusion. In theory hydrostatic extrusion can be used for both hot and cold extrusion process. However the temperature of the billet is limited by the maximum permissible temperature of the hydrostatic medium. Oils, synthetic oils, and even low melting temperature alloys are used as a hydrostatic medium. [11]

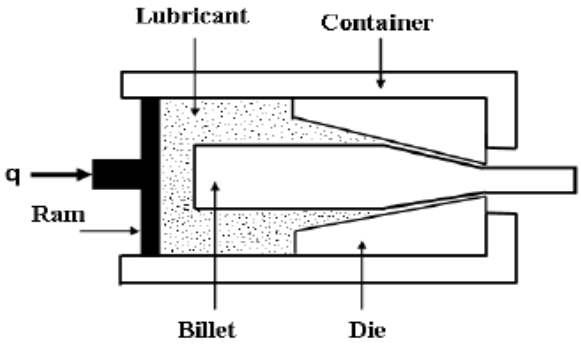

Figure 7. Hydrostatic Extrusion.

1.2.4 Continuous Extrusion

Until 1970s, extrusion has been largely thought of as a batch process, individual billets having to being fed into the containers before each stroke of the press and there being limited to the length of the extruded product. During 1960's the metal fabricators and the cable industry in particular were anxious to find a route for continuous metal forming. In conventional direct extrusion the length of the billet is limited by the frictional force generated between moving billet and stationary container which accounts for substantial proportion of the total ram force required. Investigations into hydrostatic process in 1960's and in early 1970's were aimed at eliminating billet/container friction allowing the use of longer billets. [13] Semi-continuous hydrostatic extrusion was developed to extrude billet of any length. It used the principle of augmented pressure, by which the augmented pressure is transmitted to the billet via a sealed clamping system, which along with the high pressure in the container will extrude the billet progressively. It is a batch process, as we have to stop the process as the clamp moves certain distance toward the die. This process is replaced by utilizing the dragging effect produced by high viscos liquid that flows in a continuous current past the billet in extrusion direction. High reduction is possible in one step, as there are no tensile stresses and we have high hydrostatic pressure. [14]

1.3 Continuous Rotary Extrusion

Continuous Rotary Extrusion (CRE) also known as Conform was invented in 1972 by Atomic Energy Authority in United Kingdom (UKAEA) Springfield's Advanced Metal Forming Group Laboratory. In early 1960's all extrusion process was intermittent, and the length of the billet material was controlled by the friction between container and the billet. To overcome these problems continuous extrusion was needed, CRE reversed these problem. CRE uses the friction for both feeding and to generate necessary extrusion pressure, and it is a continuous process hence length of the extrudate was not limited. CRE is preferred because it has the following advantages such as no preheating of the billet is required [11], different forms of feed materials such as powder granules, feed rod, even metal scrap from other processes can be used but all materials should be free from any contaminants before feeding into CRE. The mechanical properties are improved as we get fine microstructure in the extrudate. CRE consumes less energy when compared to other extrusion processes. Owning to circular motion CRE has some limitation such as curling phenomenon and surface separation. The major applications of CRE are production of solid and hollow extrudate profiles of non-ferrous metals: such as Al, and Cu alloys. [11] [15-18]

1.3.1 Machine Design

CRE as shown in Figure 8 consist of a rotating wheel with one or two grooves in its periphery enclosed by a shoe, a coning wheel which coins the feed stock against the groove, so that the friction between the groove and feed stock makes the feed stock move along with the rotating wheel. The deformation zone is defined by the abutment which blocks the groove, feeder plate, O-rings, die and supported by die backer. As the feed stock hits the abutment the shear

between the feed stock and rotating wheel will cause the feed stock temperature to rise and deform plastically and push it towards the deformation zone. CRE is an unlubricated process. [19]

1.3.2 Classification

The major classification of CRE are single groove, twin groove and conklad process. Single groove CRE as shown in Figure 9a is the most economical method of extruding strips, solid shapes and sections. Twin groove CRE as shown in Figure 9b has the following advantages over the single groove, more robust die can be employed, porthole can be eliminated as we can place the mandrel between the grooves in a static die holder, and the extrusion speed is higher when compared to single groove CRE. The conklad CRE process as shown in Figure 10 was developed to have temperature sensitive core to be encompassed with an aluminum tube. Conklad process is mainly used to produce fiber optic and coaxial cables where the core material will be surrounded by the conklad material. [20]

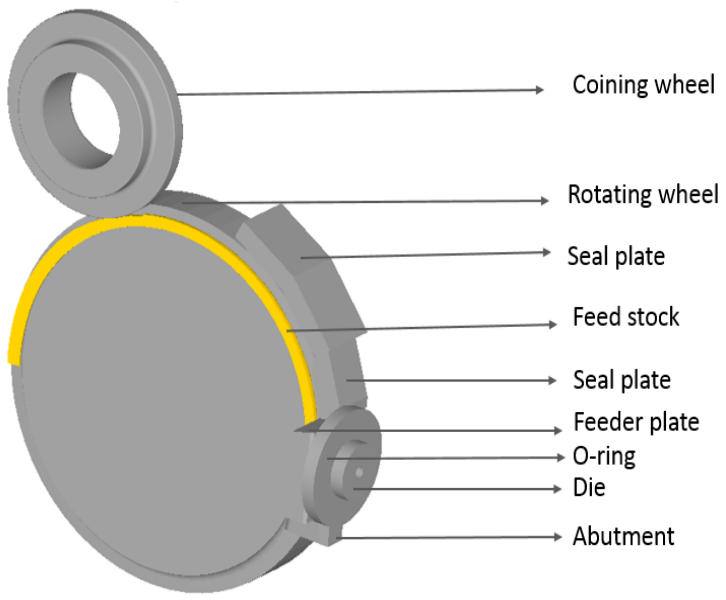

Figure 8. CRE machine design.

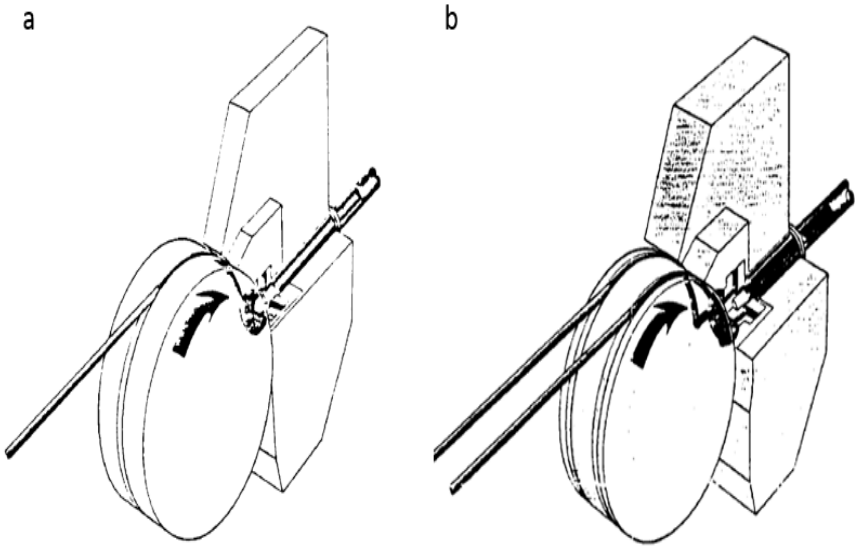

Figure 9. a) Single groove CRE b) Twin groove CRE. [20]

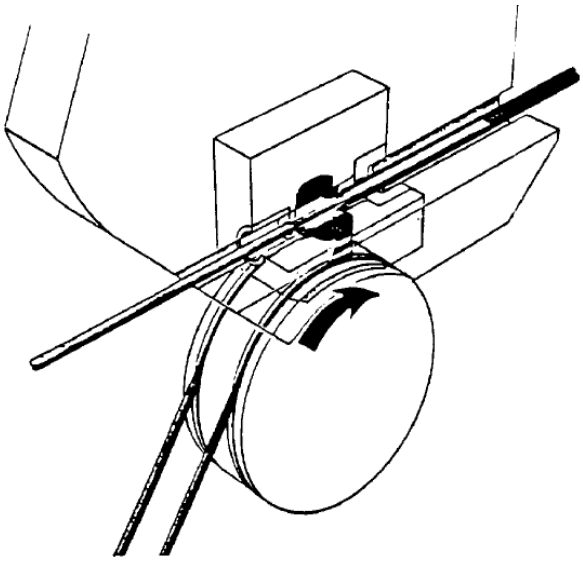

Figure 10. Conklad process. [20]

Kim Y.H et al, studied on optimal design for CONFORM process, performed set of simulation, analyzed the process parameters and proposed an optimal design. They found out that rotating wheel velocity does not have remarkable influence on material flow unless it is extremely

high. The flash gap should be minimum and increasing the lower straight part of the die should be longer relative to the upper part to result in uniform flow. [21]

Junying Yang et al. studied the effect of wheel velocity microstructure of AZ31 magnesium alloy produced by Conform process. They observed that grains are refined during the process, and at lower wheel velocity the microstructure was not homogenous and with increase in velocity the grain structure was more uniform. [22]

Monika Mitka et al, performed a CRE extrusion of AZ91 alloy at different wheel velocity they found out that the there was a huge influence of friction on the die temperature rise at higher velocity. The author also found that as the temperature increased there was decrease in strength of the extrudate but the average grain size value did not match the predictions. As the grain size decreases the strength of the material is expected to increase. [23]

From these studies it is clear that, having a reliable numerical model of Continuous Rotary Extrusion will helps us in understanding the process clearly and allow its optimization and improvement.

1.4 Flow Stress Modeling

Flow stress of a material is one of the most important parameters in metal forming. To have a good FEM model of a forming process we need to have an accurate flow stress of the workpiece as a function of strain, strain rate and temperature. Once we captured the flow stress and know how processing conditions affects the flow stress, we can develop an equation which describe the flow stress function, known as the material model or constitutive equation. [12]

1.4.1 Constitutive Equation

At low strains the stress of the material varies linearly with strain, as Hooke's law states stress σ is equal to Young's modulus (E) * (times) strain (ϵ), where σ is the stress acting on the

material. The material will starts to yield plastically when the stress in the material is increased beyond a point know as elastic limit, where the deformation will be permanent. In plastic regime the steepness of the curve between stress and strain will decrease with increase in strain as shown in Figure 11. The first model for a real metal is shown in Figure 11 and it represents the flow curve for common metals when deformed at room temperature. Due to strain hardening the true stress of the material will increase with increase in true strain. This is true for all metals commonly used in industrial forming processes such as steel, aluminum, copper, brass etc., however there are soft metals like lead, zinc and tin, whose flow stress is strongly dependent on strain rate even at room temperature. This is especially true for metal with lower recrystallization temperature which are hot deformed at room temperature such as lead and tin. Hence to simplify the mechanics, it is common to consider idealized materials like rigid-plastic or elastic-plastic material models. For such idealized material, it is assumed that there will not be any strain hardening and stress will remain constant. [12]

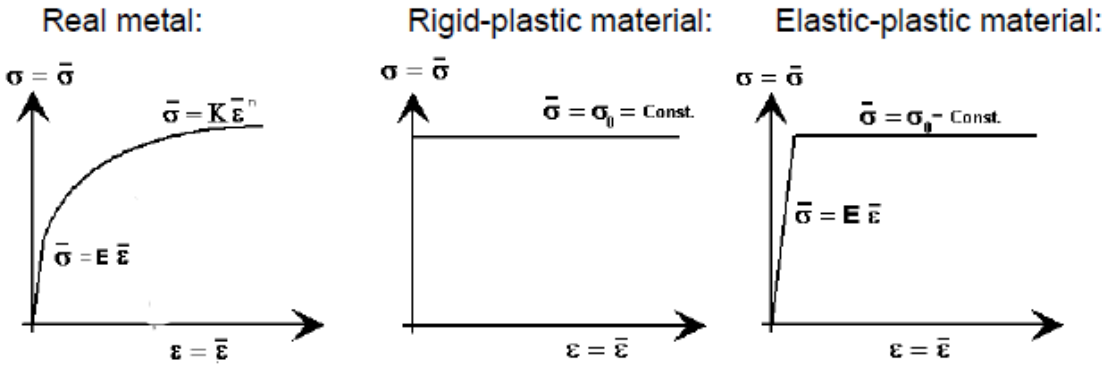

Figure 11. Flow curve for different types of materials. [12]

The flow stress condition are different for cold forming than that of hot and warm forming. Flow stress at elevated temperature depends mainly on strain rate and temperature. Under these conditions strain rate control the work hardening while temperature return controls recovery

mechanisms. Flow stress also depends on microstructure of the material which can change during the forming operation. As discussed earlier the constitutive equation is commonly used to describe the flow stress of the material and how it is influenced by the process parameters. If we take cold, warm or hot forming of common metal, strain, strain rate, temperature are the major process parameter that affect the flow stress. Therefore general constitutive equation for metals are expressed as for flow stress as a function of process parameters $\sigma = f(T, \varepsilon, \dot{\varepsilon}, S)$. If the microstructure S of the material is assumed to be constant then the expression will be reduced to $\sigma = f(T, \varepsilon, \dot{\varepsilon})$. [12]

Figure 12 shows how flow stress of aluminum alloy depends on temperature and strain rate. At very low temperature (room~100 degree Celsius) i.e., cold forming operation the flow stress is high and does not vary with temperature. Strain hardening is observed in cold forming, the flow stress will increase with increase in strain. If the work piece material is heated above recrystallization temperature, which is 0.6*melting temperature of the material in Kelvin scale i.e., when hot forming is performed the flow stress will be reduced to five to tenfold, indirectly reducing the forming load. In Figure 12 the boxes CF, WF, HF, represents cold forming, warm forming, and hot forming respectively for aluminum alloy. For some material there might be jumps in flow stress caused by temperature changes due to material phase change. [12]

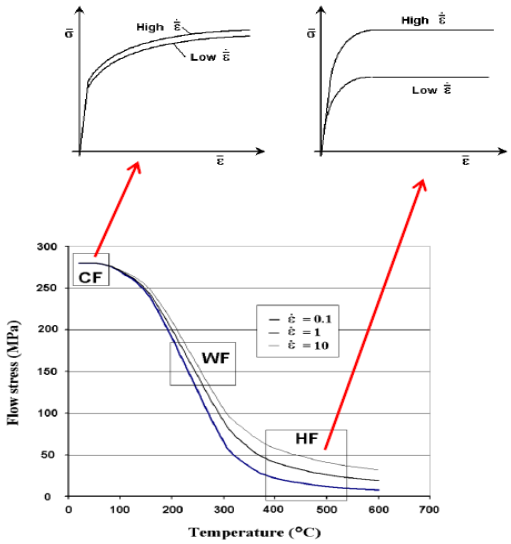

Figure 12. Typical aluminum alloy flow stress dependence of temperature and strain rate. [12]

1.4.2 Material Constitutive Model

1.4.2.1 Norton-Hoff Equation

Norton-Hoff equation is commonly applied to describe flow stress data for cold, warm, and hot forming. The equation is as follows:

$$\sigma = K\varepsilon^{n}\dot{\varepsilon}^{m}e^{\beta/T} \quad [1]$$

Where, k, n, m, and β=Q/R represents material-dependent constants that can determined by curve fitting from experimentally calculated flow curves. These constants are named as K-strength coefficient, n-strain hardening exponent, m-strain rate sensitivity and β is temperature sensitivity. In cold forming the flow stress is not affected by the strain rate, or temperature if temperature rise is moderate as shown in Figure 12, hence the Norton-Hoff equation is reduced to a simple form as shown in equation 2. [12]

$$\sigma = K\varepsilon^{n} \quad [2]$$

1.4.2.2 Power Law

During warm forming where the temperature is at intermediate range, the flow stress depends on strain, strain rate, and temperature at this situation we can use Norton-Hoff equation. During hot forming the strain hardening effects often become negligible due to microstructural changes caused by recovery and recrystallization, and the flow curves become straight at high strain levels. In this case we can use power law equation which is as shown in equation 3.

$$\sigma = C\varepsilon^{m} \text{ [3]}$$

If there is significant change in the temperature then the equation changes to the following term as shown in equation 4, to adjust for material recovery mechanism. [12]

$$\sigma = C\dot{\varepsilon}^{m} e^{\beta/T} \text{ [4]}$$

1.4.2.3 Zener-Hollomon

Zener Holloman relation is commonly used to describe the flow stress of the material in hot forming alternative to power law. It expresses the flow stress in hyperbolic-sine law as shown in equation 5.

$$\sigma = 1/\alpha \sinh^{-1}\left[\left(\left(\dot{\varepsilon}^{m} e^{Q/RT}\right)/A\right)^{1/n}\right] \text{ [5]}$$

Where: Q- activation energy, A- material constant. [12] [27].

An experiment was performed by C. Zener and J.H Hollomon to check the equivalence of the effects of changes in strain rate and in temperature upon the stress-strain relation in metal, and also found that this equivalence was valid for steels. They also concluded that they can predict the material behavior at higher strain rates and temperature through this equivalence. [24]

Takuda et al. in his work expressed a simple form of temperature compensated strain rate, i.e. Zener-Holloman expression for the evaluation of flow stress of Magnesium based alloy AZ31 and AZ91 in hot working process. In this work they did not considered strain effect on flow stress as at elevated temperature the strain hardening effect is insufficient. [25]

Z.Q. Sheng, R. Shivpuri in their work developed a Zener Hollomon flow stress model for Magnesium alloy AZ31 at elevated temperature and compared it with three published experimental data and found out that their predicted flow stress curves match well with those data. [26]

Based on the above studies we can state that the Zener Hollomon model fits the flow stress of Magnesium alloys at elevated temperature.

1.5 Finite Element Analysis

The first effort to develop the Finite Element Method (FEM) dates back to 1941-1942. The method was further developed over the decades and given a mathematical foundation in 1973. FEM is a numerical method of finding approximate solutions for partial differential and integral equations. The first method was based on energy principle such as virtual work or minimum total potential energy and it was applied to structural mechanic analysis. Today the prediction of stresses and displacements in mechanical objects and systems, and in other applications are done by Finite Element Analysis FEA. 3D models developed by the computer aided design software today will give more accurate results. FEA allows entire design to be constructed, refined, and optimized before parts are manufactured, this has significantly improved the standard of engineering design and the methodology of the design process and reduced the time substantially required to get products from concept level to production line in many industrial applications. [12]

The recent advancement in Finite Element Analysis, and with increasing use of powerful computers made it possible to simulate the metal forming process at various stages. Now a days there has been an increased use of FEA, since a FEA model for a forming application can predict the load requirement, velocity, strain rate, strain and stress fields etc., which can be used to optimizing of the process. [12]

There are three important goals for performing FEA analysis of metal forming process. Frist, the analysis aims to reduce the trial and error in tool and process design. Second, analysis is useful in designing desired parts for ease of manufacturing. Finally if there is a problem in the process, it can be handled easily. Analysis helps us to study the material flow, load calculations, as temperature distribution. We can completely plot and understand the process, reduce the lead time and improve the product quality at minimum cost. [12]

In the past most of the metal forming technology, was designed by a costly trial and error experimentation as the predictions of material flow and forming loads, depended mainly upon the experience and intuition of the metal former/designer. This costly process may be avoided by the use of numerical simulation to better understand the mechanics of the forming operation. Numerical modeling techniques analyze a process numerically with the help of mathematics. The numerical modeling are usually validated by comparing with measured data, such as the shape change or the required forming load. [12]

It is also difficult for an analytical solution of temperature, stress, strain, and strain rate distribution for extreme nonlinear conditions caused on the deformed body by large strains, plastic flow of anisotropic materials, with interfacial friction between irregular-shaped surfaces under changing contact, and hence FEM is used to assist understanding of the local conditions. [12]

1.5.1 FEM Modeling Approach

In FEM modeling, a collection of subdomains called finite elements makes the work piece as shown in Figure 13. The elements are bounded by sets of nodes, which define the localized mass and stiffness properties of the model. The equations of equilibrium along with applicable physical considerations such as compatibility and constitutive relations, are applied to each element to construct a system of equations, then the system is solved using advanced numerical techniques. The accuracy of the FEM method can be increased by increasing number of elements. However the quality of the solution is directly dependent on the quality of the material model.

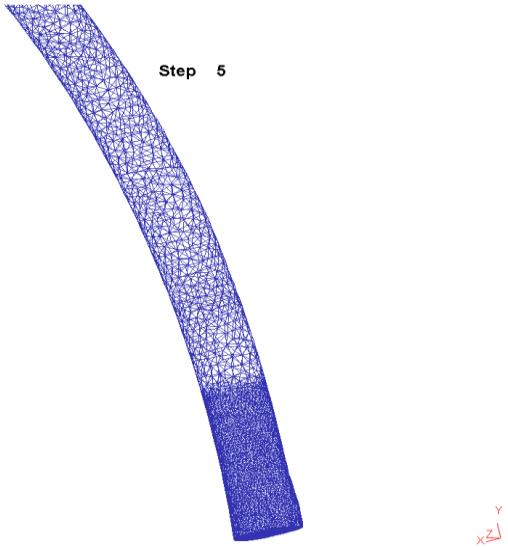

Figure 13. Meshed work piece as used in numerical modeling of CRE process.

To obtain a solution using FEM approach we have to perform five steps, 1) define elements, 2) establish the equation for those elements, 3) find elements' properties, 4) obtain a set of equation by assembling elemental equations, 5) solve this set of equation by numerical technique. [12]

To perform an FEM simulation we have to select proper deformation description, solution procedure, types of flow formation, material model and remeshing, based on requirements of our material and deformation process.

1.5.1.1 Deformation Description

There are two modes of deformation description, they are the Lagrangian and the Eulerian. In Lagrangian the nodes move along with the material, hence remeshing is required. Lagrangian method is used when the material flow is not constant. While in Eulerian the nodes are fixed and does not need remeshing as the element do not change the shape. Eulerian can be used when there is a constant material flow. There are many software packages offer these two description, for example DEFORM has these two option. [12]

1.5.1.2 Solution Procedure

There are two solution procedure they are known as explicit and implicit solutions. The implicit procedure requires lot storage and CPU time, as it uses automatic incrementation strategy to solve a large system of equations. Explicit methods are easier to calculate the solution, as they use fewer control parameter. Implicit method is also effective and can be faster in solving smaller problems. While working with a problem with large, refined meshes, explicit method is more effective. [12]

1.5.1.3 Flow Formation

In case of metal forming elastic strain is negligible when compared to the plastic strain hence the workpiece is considered as rigid-plastic or rigid-viscoplastic, and the flow formation is based on Levy-Mises flow rule. If elasticity cannot be ignored then the material is considered as elastic-plastic or elastic-viscoplastic solid. In this case the flow formulation is based on Prandtl-Reuss equation. [12]

1.5.1.4 Material Model

In order to run a simulation, we must specify the flow stress curve of the workpiece used. There are different material models available such as Power-law, Zener-Holloman, Norton-Hoff model etc. Based on our process we have to select a model which agrees well with our material behavior. We can also directly input the function $\sigma = f(\varepsilon, \dot{\varepsilon}, T)$ in terms of the flow curves for a given material, where the software will interpolate between the given data points. [12]

1.5.1.5 Remeshing

In FEM analysis, there might be large errors due to finite elements distortion. To overcome this problem the finite element must be remeshed periodically. There are two types of remeshing method, i.e., adaptive remeshing and static remeshing. Adaptive remeshing allows larger deformation without any intervention by the user. While static remeshing is less automatic, it avoids excessive error that occur in adaptive remeshing and requires less calculation. In process where metal deforms severely must be remeshed frequently to get better results. [12]

1.5.1.6 DEFORM™ FEM Software Package

DEFORM™, FORGE™, SUPER-FORGE™, Q-FORM™, ANSYS™, and ABAQUS™ are some of commercial codes that are available, with most of them designed specifically for bulk-metal forming applications.

The DEFORM™ software has been proved to be accurate and robust in industrial application. We can have an enhanced resolution of part features, while maintaining the overall problem size and computational requirements, as DEFORM™ generates an optimized mesh system with local element size dependent on the processes to be analyzed by automatic mesh generation. The user can also manipulate mesh density locally at different parts by having a

separate mesh window to meet their requirement. The software provides sophisticated analysis capabilities, and the graphical user interface is intuitive and easy to learn. [12]

DEFORM^{TM} software was acknowledged by the several Benchmark edition at the Institute of Forming Technology and Lightweight Construction (IUL) of Technische Universität Dortmund, Germany in cooperation with the DIEM of University of Bologna, Italy. In the Benchmark study a very challenging experiment was set up to record the relationship between material flow, die deflection, and profile distortions and it was parallel modelled by various software people and compared to the experimental data . [28]

1.6 Folding Defects

In case of not optimized metal flow conditions some defects known as laps or folds can be created. If there is a whirl (w) type material flow present, it may cause over folding of metal as shown in Figure 14 b and 14 c. It is difficult to detect folding defect by visual inspection, however it can been through metallographic analysis. Occurrence of this defect is unacceptable as it causes the component to facture during the use. This defects can be eliminated by modifying the process conditions including changes in the die design as shown in Figure 14 a. [12]

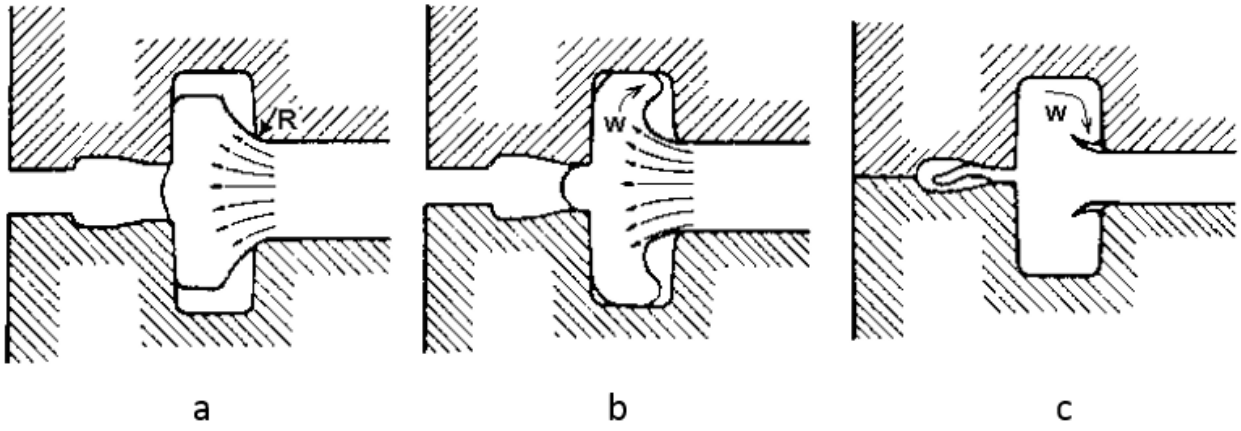

Figure 14. Whirl type of metal flow creating over folding. [12]

2 FEM-MODELING OF CRE PROCESS

The commercial software DEFORM-3D™ was used to simulate the continuous rotary extrusion (CRE) process. During numerical modeling it was also assumed that: workpiece is modeled as plastic material, tools were modeled as rigid material, friction factor between the workpiece and the tool was constant and the thermal characteristics of the workpiece and the tool was constant. Direct extruded rod of 10 mm diameter as shown in Figure 15 was used as input work piece. Figure 16 show the continuous rotary extrusion geometry. The work piece is placed inside the groove in the rotating wheel. All the parts that are not be direct contact with the work piece were removed to make the model clearer. After doing that the model looks like as shown in Figure 17. The model consists of rotating wheel with a groove, abutment, feed plate, O-ring, die, seal plate, coining wheel. Various parts are shown in Figure 18. Typical steps involved in CRE such as coining, upsetting, filling, extrusion are shown in Figures 19, 20, 21, and 22 respectively.

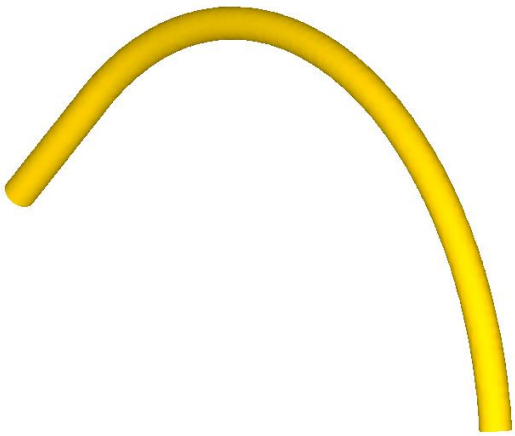

Figure 15. Work piece.

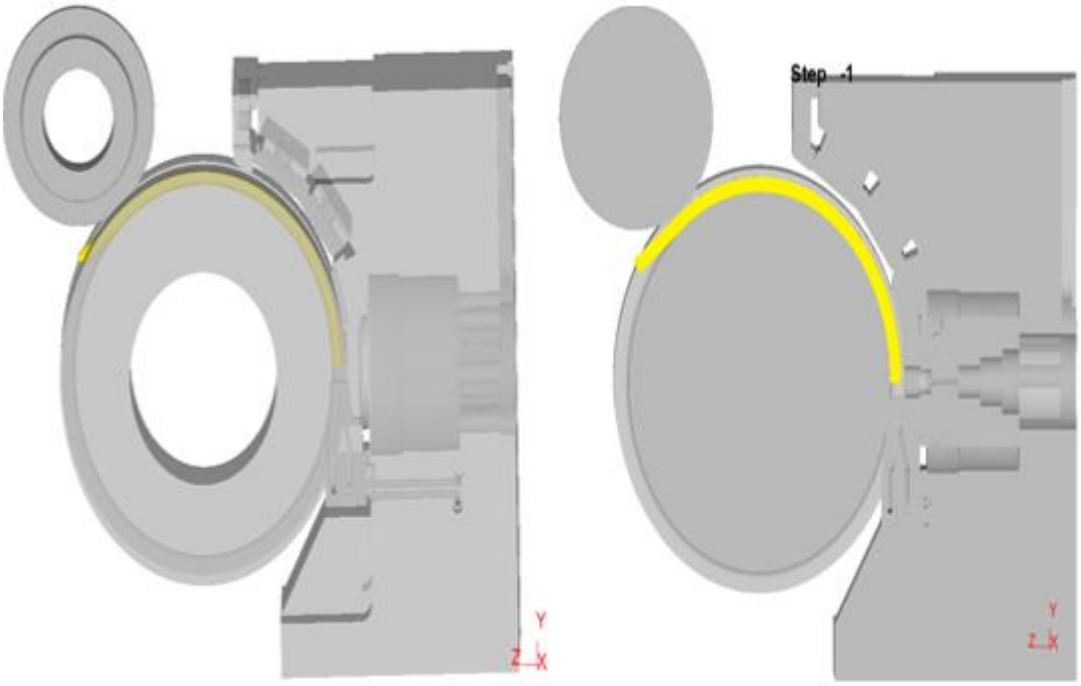

Figure 16.Continuous Rotary Extrusion (CRE) Geometry.

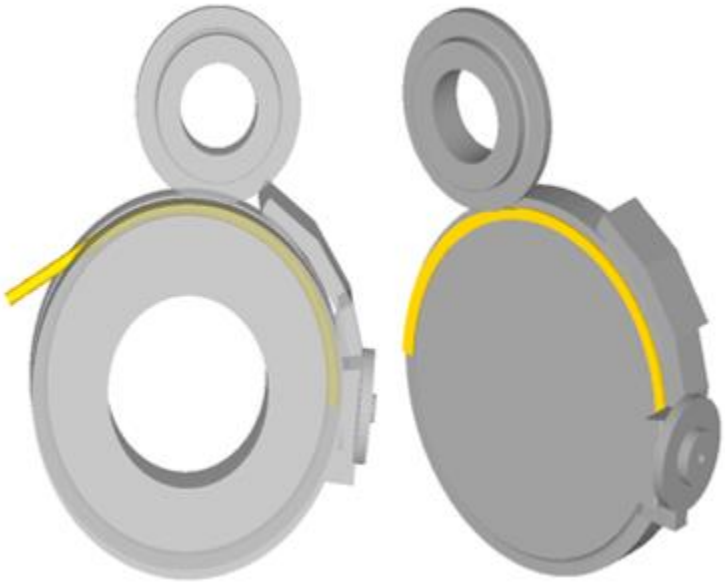

Figure 17. New model consisting of essential parts of the CRE process.

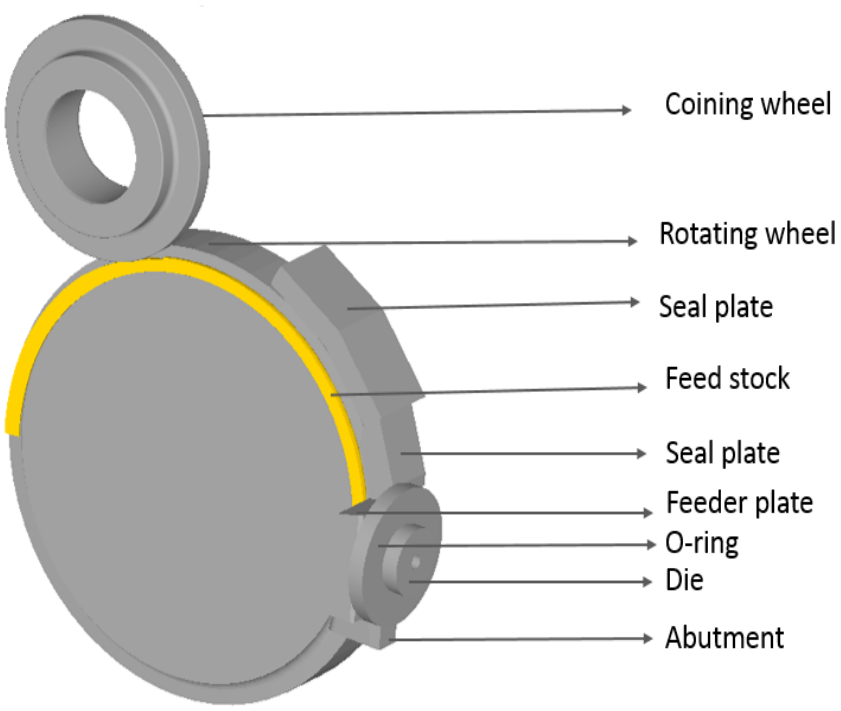

Figure 18. Parts characteristic in the CRE process.

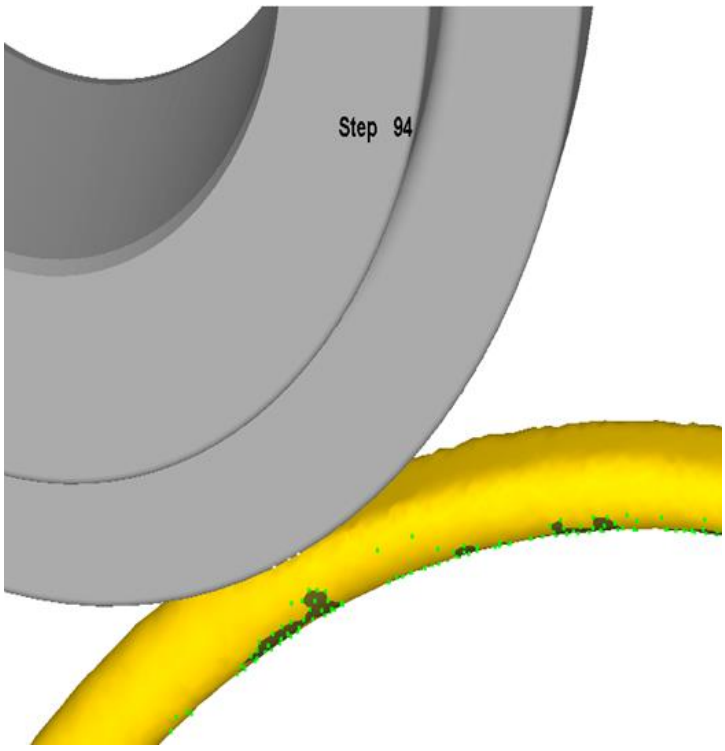

Figure 19. Coining process.

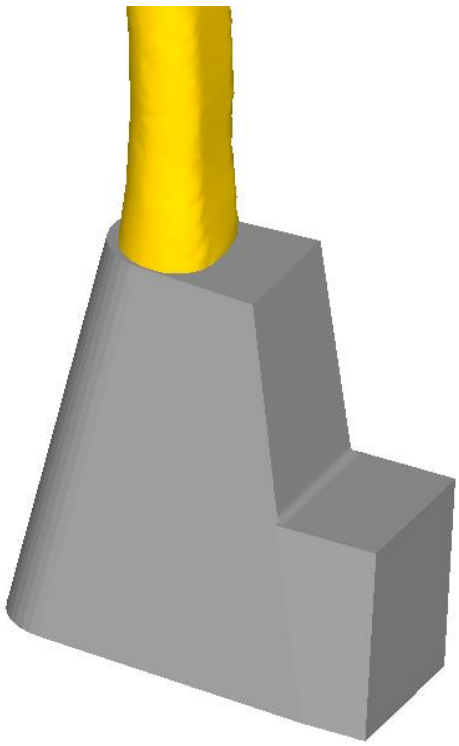

Figure 20. Upsetting stage.

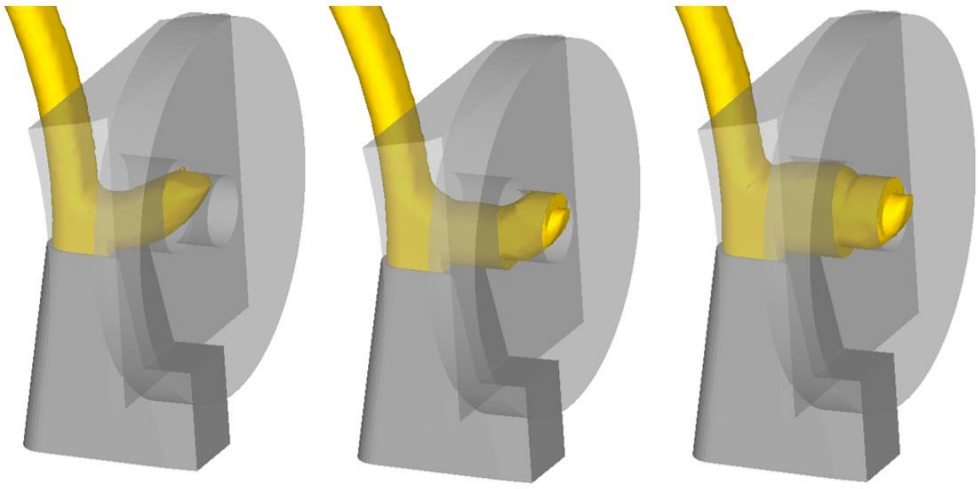

Figure 21. Stages of filling.

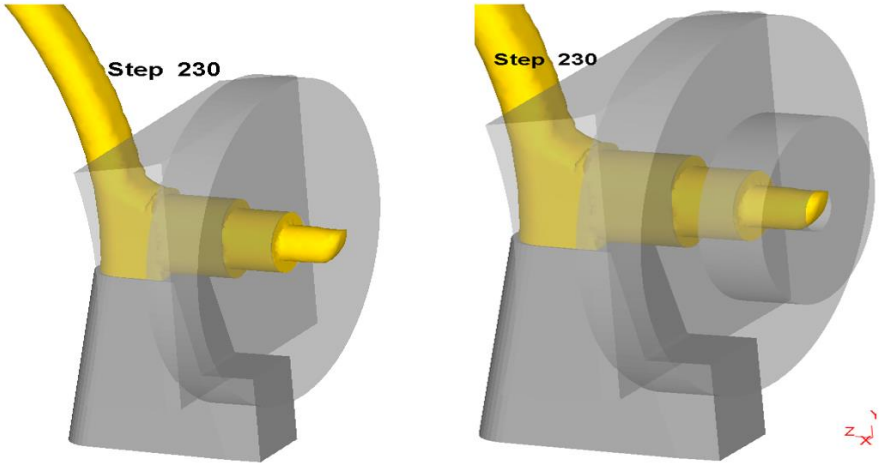

Figure 22. Extrusion through die.

At first to check whether this model was working, Aluminum alloy Al6061 was chosen as the work piece material for the initial proof of the concept study since it was already modeled using the software and tooling material was chosen as AISI-H-H13. A friction factor of 2 between the rotating wheel and work piece was selected, while a friction factor of 0.7 was used between the feed plate, O-ring, die and work piece and for all other material which are in contact with the feed stock a friction factor of 0.1 was used. The rotating wheel was rotated at 0.19 rpm. The feed plate was assigned a temperature of 400° C, O-ring and die was assigned a temperature of 500° C to make the metal flow easy, and all other are kept at room temperature of 20° C at the beginning of the simulation.

2.1 Model improvements

2.1.1 Leakage

During running of the first model, it has been noticed that as the feed rod hit the abutment and started to deform plastically there was some materials slipping from the feed rod into the gaps on the sides of the abutment as show in Figure 23. As the result of this there was not enough feed rod material to flow into the die and enter on the other side of the machine, it stopped the metal

flow within the deformation zone itself. This happened abutment upsetting surface was small and there was a gap between the rotating wheel and the abutment. To reduce this leakage the mesh size was reduced and also abutment size was improved and kept in a position so that it had no gap between the abutment and rotating wheel as shown in Figure 24, and 25. Figure 26 shows the comparison between old and adjusted models, with different mesh size no leakage is noted for the adjusted geometry.

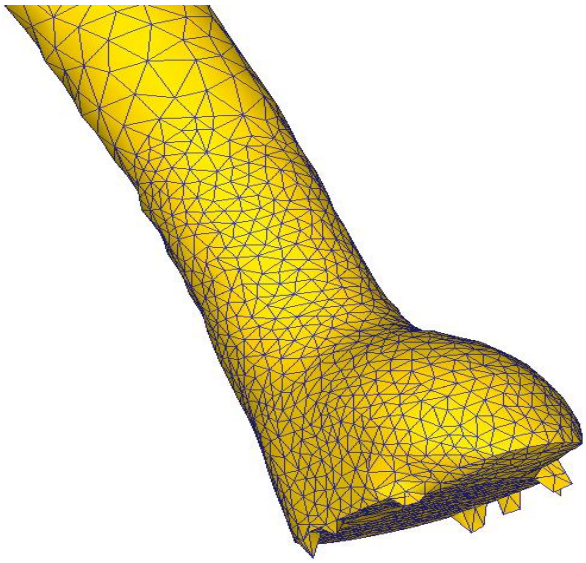

Figure 23. Node Leakage.

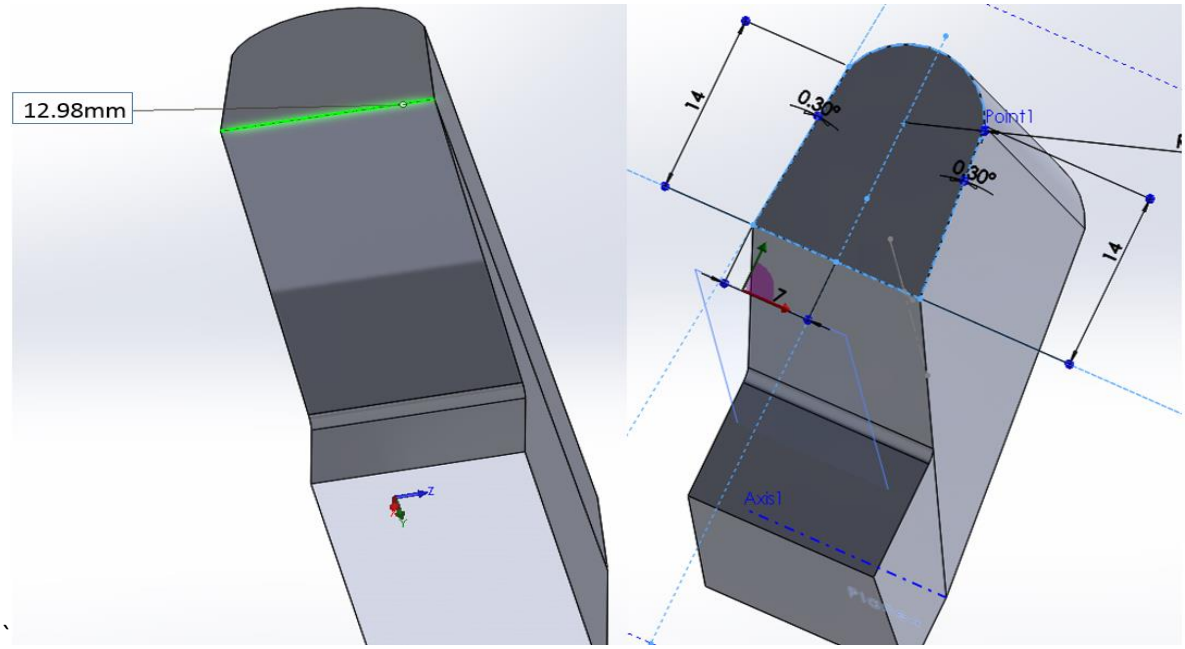

Figure 24. Adjustment of the abutment size.

As shown in the Figure 24 green highlighted length was increased from 12.98 mm to 14 mm.

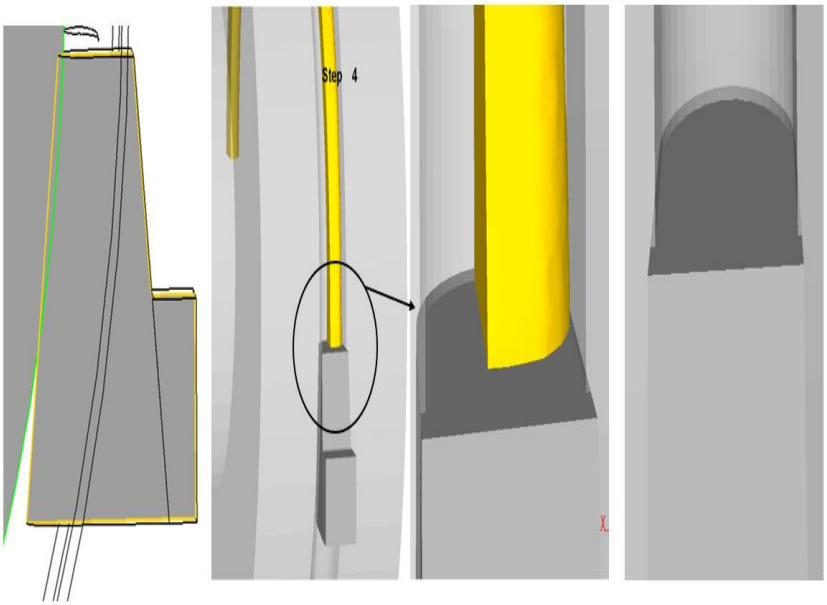

Figure 25. Placement of the abutment so that there is interference b/w rotating wheel and abutment.

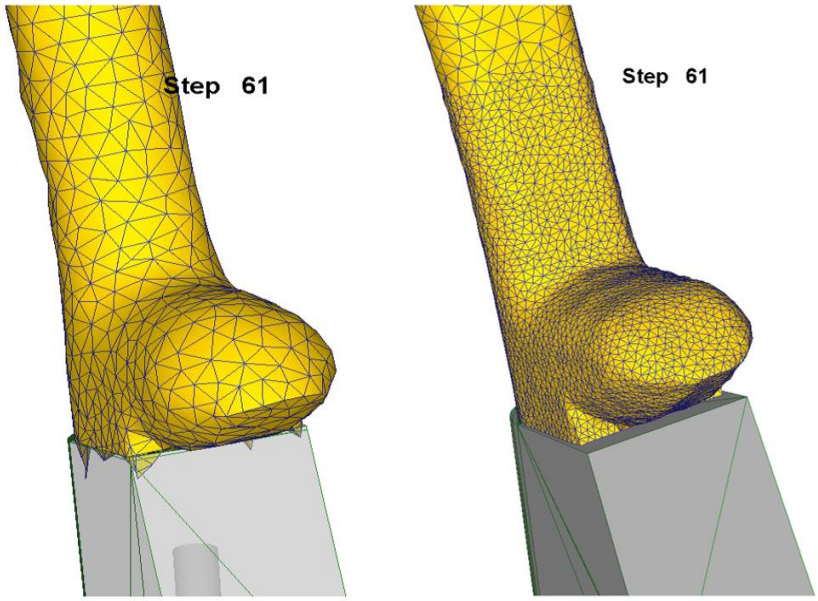

Figure 26. Old model vs improved model.

2.1.2 Contact

The contact at the beginning of the process was not enough as shown in Figure 26 (the green point in Figure 27 represents the nodes of the work piece in contact with the rotating rod) and as the feed rod moves away from the coining wheel further down, feed rod losses contact with groove in the rotating wheel as shown in Figure 28, as a result of which the rotating wheel simply moves without applying any force on the feed rod as the feed rod just slips from the groove.

Coining by coining wheel: The main reason for very low contact is that there is no proper coining of the work piece is done as you can see Figures 27, 28, and 29 the feed rod remains its circular shape it is not pressed down against the groove. To fix this problem the longer rod is used, with proper coining operation as shown in Figure 30, so that there is desired contact.

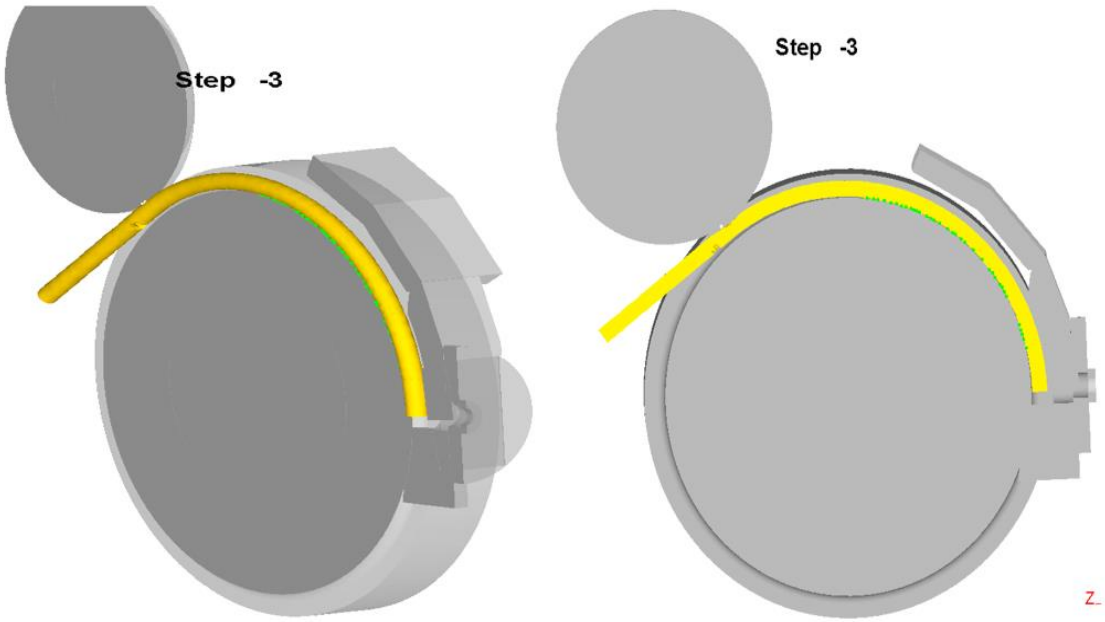

Figure 27. Contact b/w feed stock and rotating wheel.

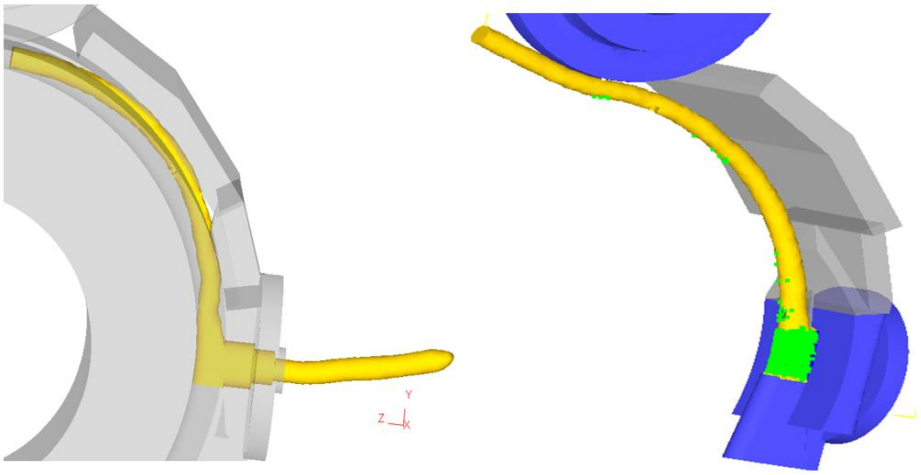

Figure 28. Loss of contact b/w work piece and rotating wheel.

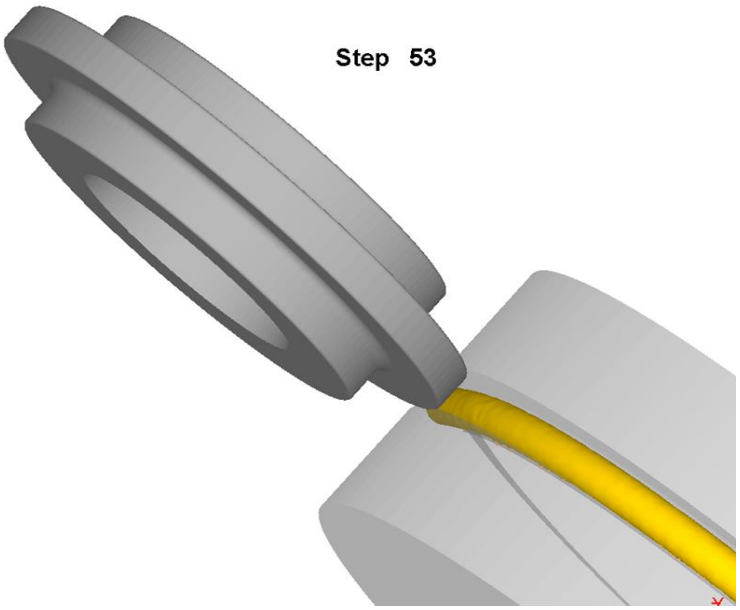

Figure 29. Improper coining.

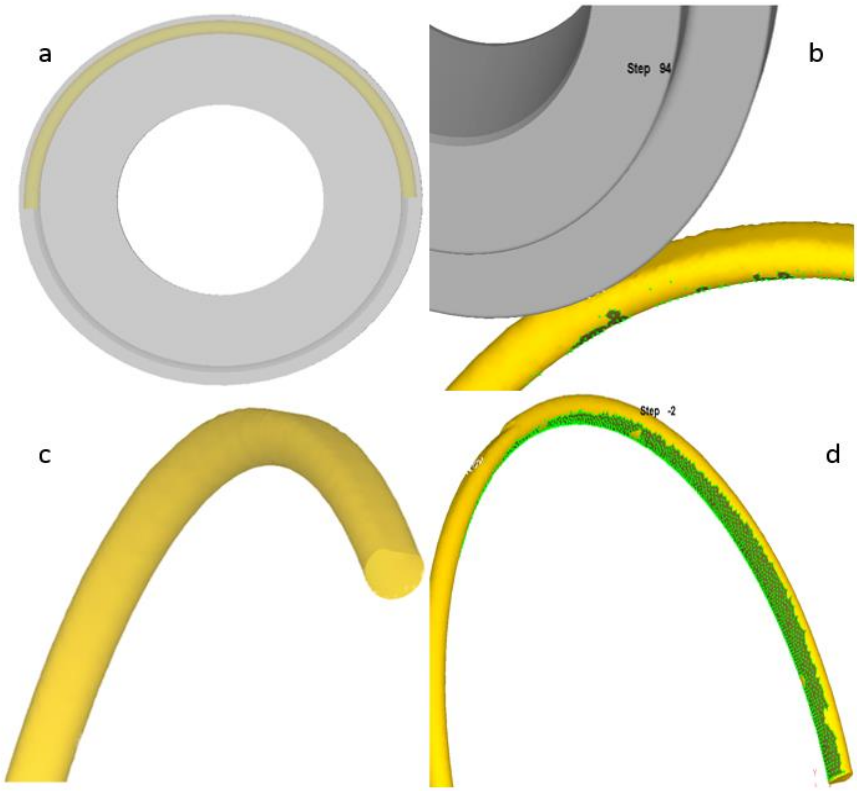

Figure 30. a) Increased length of work piece, b) Proper coining, c) Properly coined work piece, d) Improved contact.

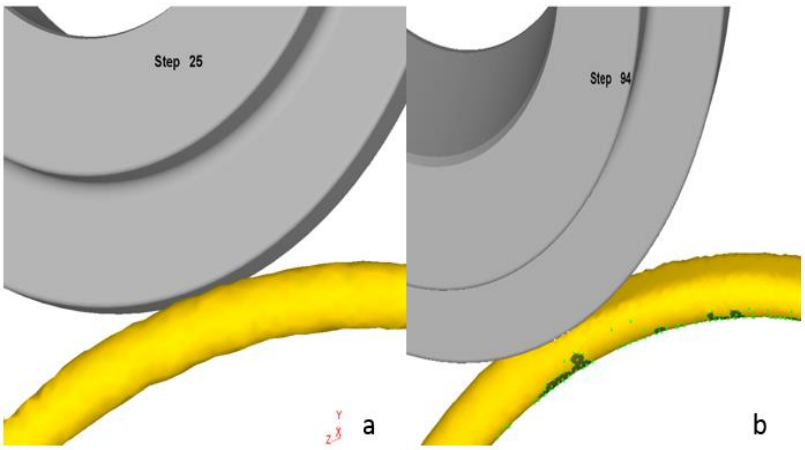

Figure 31. a) Improper coining, b) Proper coining.

Coining by compression: Proper coining operation was achieved by having the starting end of the work piece pressed down (flatten) up to a particular length, against the groove by a compression tool as shown in Figure 32a. As we can see from the Figure 32b, the compression tool will press the work piece against the groove in the rotating wheel as it move towards center of the rotating wheel. While doing this the front face of the work piece was fixed so that the material is moved in the reverse direction not towards the deformation zone to keep the front face which will upset the abutment to be flat as we can see in Figure 30c.

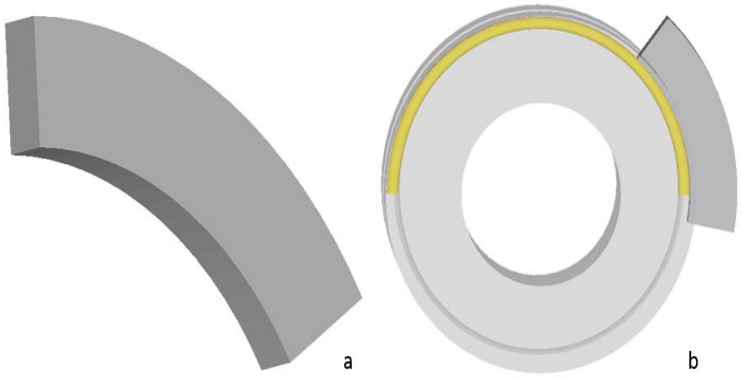

Figure 32. a) Compression tool, b) Compression process.

Additional help tool shown in Figure 33 was also used to prevent the work piece from losing contact. There was no inter-object relation between the help tools and the work piece, i.e., there is no heat transfer or any kind of interaction between the help tools and work piece, and friction between them is also set as zero. The main function of these help tool is to prevent the work piece from moving out of the groove and lose contact. The help tools do not simulate the physical process.

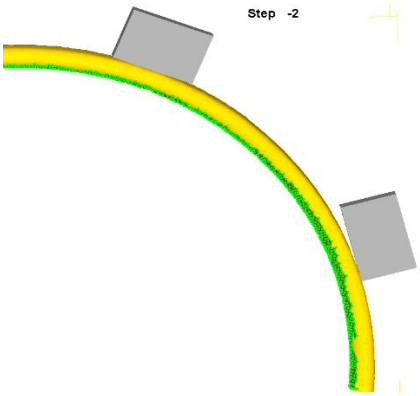

Figure 33. Help tools to maintain contact b/w work piece and rotating wheel.

2.2 Models

Now that the process model is improved simulation of Magnesium alloy extrusion can be performed. Four different models were developed with different extrusion ratios, billet temperatures, tool temperatures as shown in Table 2. The cell which are highlighted in green in Table 2 are the parameter changed in the models.

Table 2. Description of Models. [29]

Model No	1	2	3	4
data for the numerical simulation				
wheel diameter (mm)	265	265	265	265
work piece diameter (mm)	10	10	10	10
wheel speed (rpm)	3	3	3	3
extrusion ratio	1.25	1.25	1.11	2
material data				
material work piece	AZ91	AZ91	AZ91	AZ91
material tooling	AISI-H13	AISI-H13	AISI-H13	AISI-H13
Thermal Conductivity (N/Cs)	84	84	84	84
Heat capacity (N/Cmm^2)	2.096	2.096	2.096	2.096
Heat transfer Coefficient (N/Csmm^2)	22	22	22	22
emissivity	0.12	0.12	0.12	0.12
Friction factor b/w material and wheel	0.9	0.9	0.9	0.9
Friction factor b/w material and abutment	0.6	0.6	0.6	0.6
Friction factor b/w material and seal plate	0.3	0.3	0.3	0.3
Friction factor b/w material and other tools	0.5	0.5	0.7	0.7
Work piece initial temperature C	350	20	20	20
Wheel temperature C	100	100	20	20
Feed plate, O-ring temperature C	100	100	500	500
Die temperature C	200	200	350	350
Abutment temperature C	100	100	100	100
other tool temperature C	20	20	20	20

Simulation parameters				
No of Mesh elements for work piece	68295	68295	68295	68295
Time steps (s)	1	1	1	1

2.2.1 Friction model

Tresca friction model as described in equation below was used

$$\tau = m*k \quad [6]$$

Where, τ - Frictional stress, m - Friction factor, k - Shear yield stress. The friction between the workpiece and the tool is assumed to be constant. [12]

2.2.2 Material Model

Flow stress data of AZ91 Magnesium alloy was obtained from a paper "Flow stress modeling of AZ91 Magnesium alloy at elevated temperature by Raghunath et al [4]. In their work the authors used the compression test results to construct the flow stress curves and also proposed an analytical model for constructing the flow stress model. They also studied the dependence of flow stress on deformation temperature at various strain rates in detail by plotting the flow stress at a strain of 0.3 as shown in Figure 34.

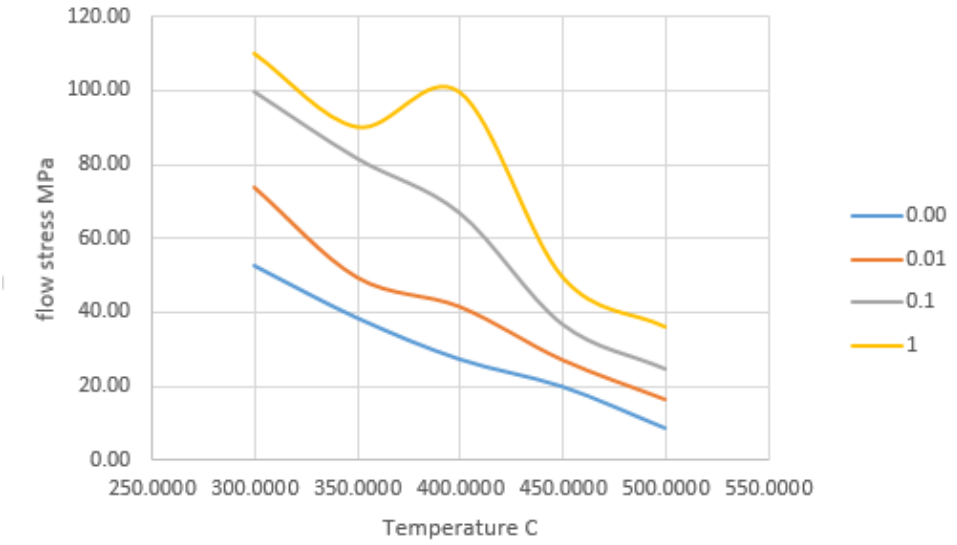

Figure 34.Dependency of flow stress at strain of 0.3 on deformation temperature at various strain rate.

The Zener-Hollomon parameter, which is expressed as hyperbolic-sine law as shown in equation 5 is often used to describe the relationship between the strain rate, flow stress, and temperature. It was used as a material model. [12] [27]

$$\sigma = 1/\alpha \sinh^{-1}\left[\left(\left(\dot{\varepsilon}^{m} e^{Q/RT}\right)/A\right)^{1/n}\right] \text{[5]}$$

Where, σ is the effective flow stress, ἐ - strain rate, Q - activation energy, T – absolute temperature, R - gas constant, and A, α, n are material constant. Regression analysis [31] was made on the data obtained from the paper [4], and the values of A, α, Q, and n are found as 2.52E+09, 0.030886713, 155088.8951, 3.740245027 respectively. As shown in the Figure 20 the regression coefficient R^2 is found to be 0.9298, hence there is a very good approximation between the experimental data from the paper and model. Hence based on the relationship presented in Figure 35 we can state that Zener-Hollomon model can be used for Magnesium AZ91 alloy to relate the flow stress to the deformation temperature and strain rate.

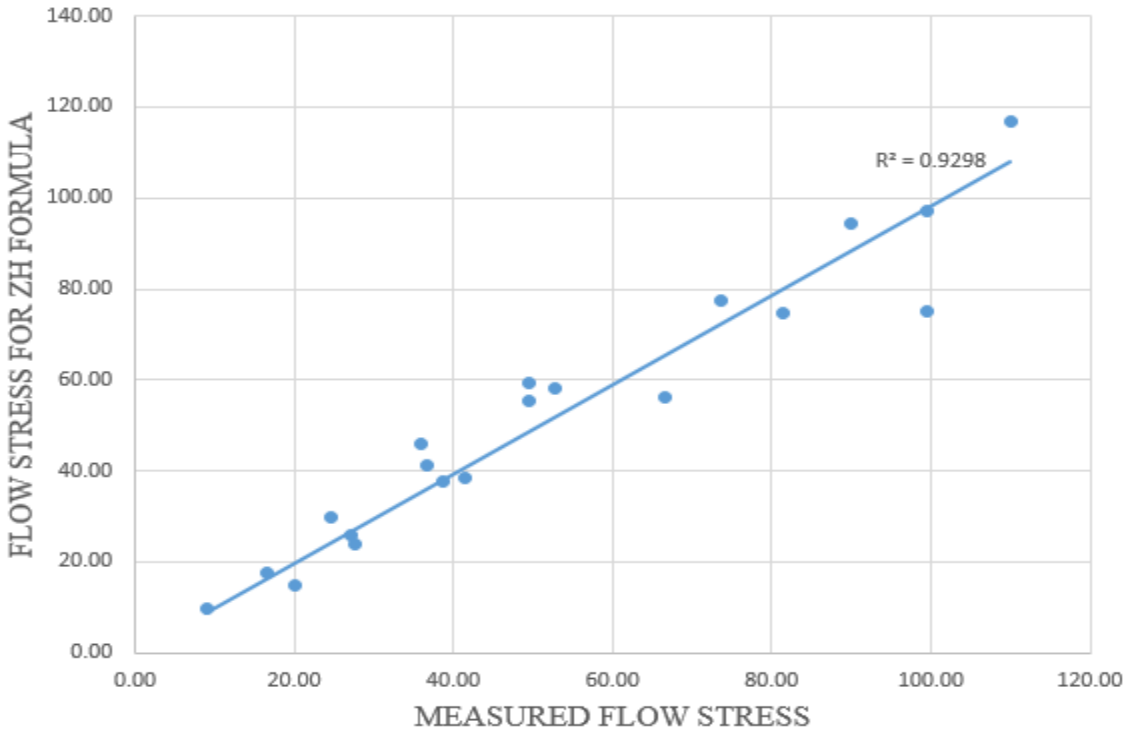

Figure 35. Dependence of flow stress at 0.3 strain on Zener Hollomon.

Figure 35 shows the flow stress graph generated by the DEFORM 3D software using the Zener Holloman material model that is inputted into the software. It has a strain rate range of 0~5 s^{-1} and temperature range of 20~1400 C, of course the simulation uses data less than the melting point of the magnesium. The thermal and frictional characteristics of AZ91 Magnesium alloy are assumed to be constant as given in the Table 2.

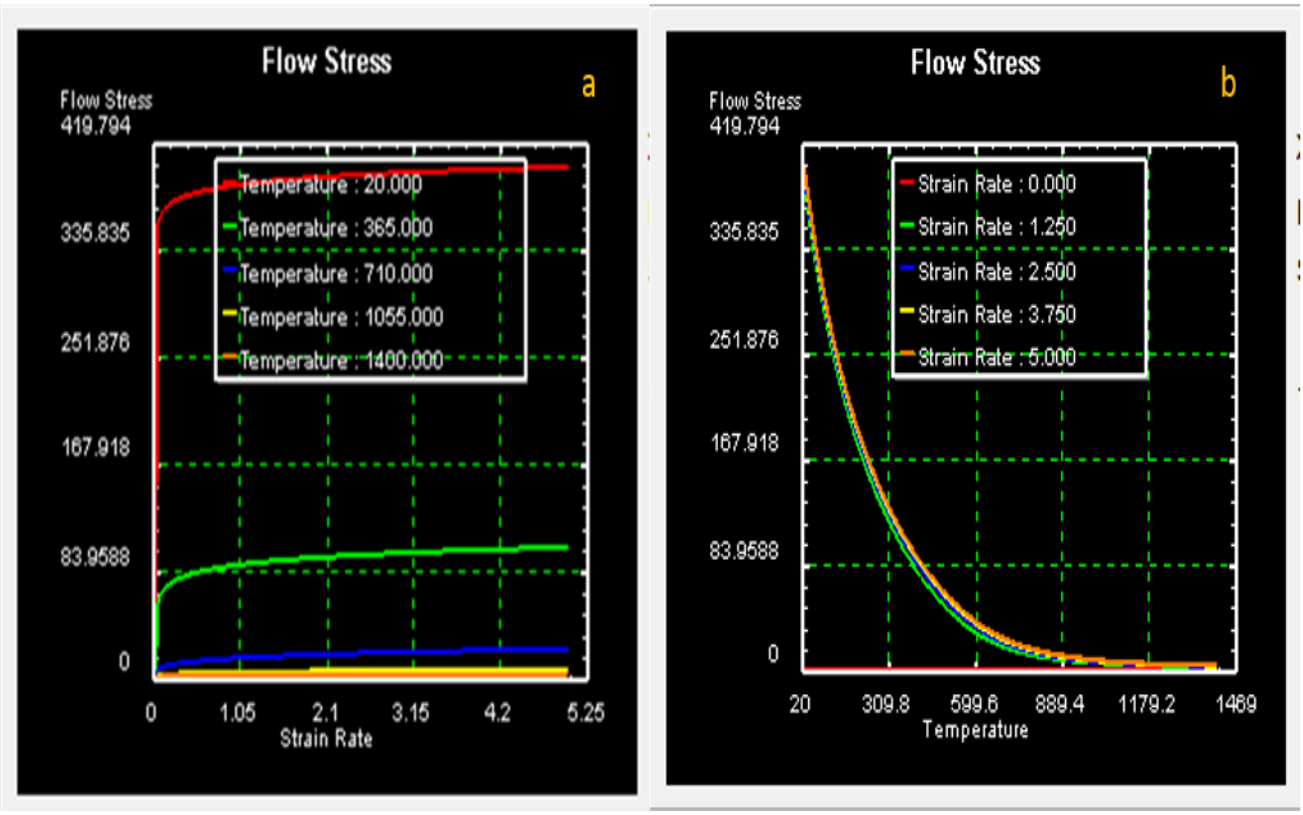

Figure 36. a) Flow stress vs Strain rate at different temperatures. b) Flow stress vs Temperature at different strain rates.

3 RESULTS

3.1 Model 1

Different models were used to present different process conditions for CRE according to Table 2. All comparison between the models are made at same time step of the simulation, t = 21.5 sec. Figure 37a shows the results for extrusion using model 1. The buildup is caused as a result of plugging of the metal in the deformation zone, as it can be seen from the Figure 38. The velocity in the deformation zone i.e., inside the feeder plate, O-ring, and then die is almost zero, causing plugging of material in the deformation zone which in turn act as a blockade for the soft material which is fed by rotating wheel. Hence as shown in Figure 38 the material starts to buildup

in the upper direction. Strain rate measurement also confirmed that the material in the deformation zone is almost dead i.e., there is no movement as shown in Figure 39.

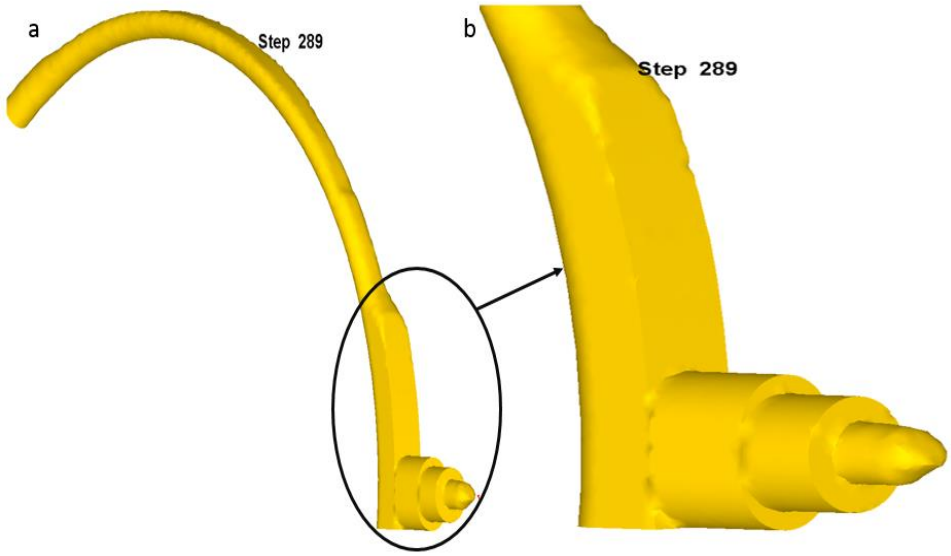

Figure 37. a) Model 1 Extruded profile. b) Buildup formation.

This problem is caused by the low deformation zone temperature, as shown in Figure 40 the temperature of the feed plate, O-ring and die is almost equal to 100º C, which increase the material flow stress in the deformation zone making it harder to deform. The workpiece temperature in the buildup region is a 300 º C which make it softer and easily deformable hence the material builds up. High temperature workpiece and low temperature deformation zone also helps in this buildup phenomenon, as there will be heat transfer taking place between the workpiece and deformation zone material which will cool down the work piece material in the deformation zone causing it to plug, as set upped in this case model 1.

In addition to this the rotating wheel temperature is also important because it can heat up the material in the groove and making the work piece softer in the groove will also leads to this buildup phenomenon. As one can see in Figure 40a the workpiece which is in the groove end is heated up making it softer and the workpiece material, which is on the other end is at lower

temperature because of the heat transfer between the work piece and the seal plate. This effect is can be clearly seen in Figure 39 strain rate is higher in the workpiece material which is inside the groove of the wheel as material is soft and there is a dead metal zone in the other end.

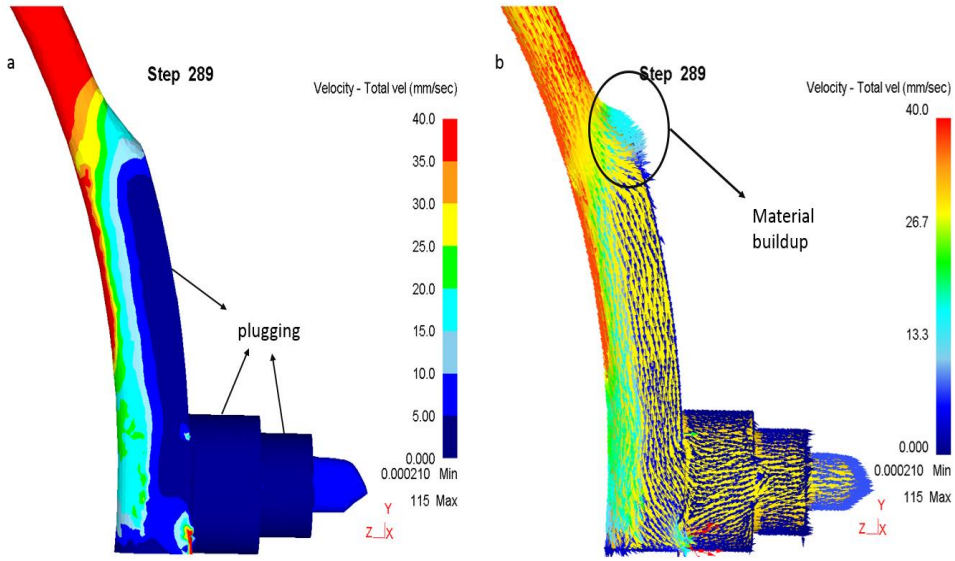

Figure 38. a) Velocity at the deformation zone, b) Material buildup.

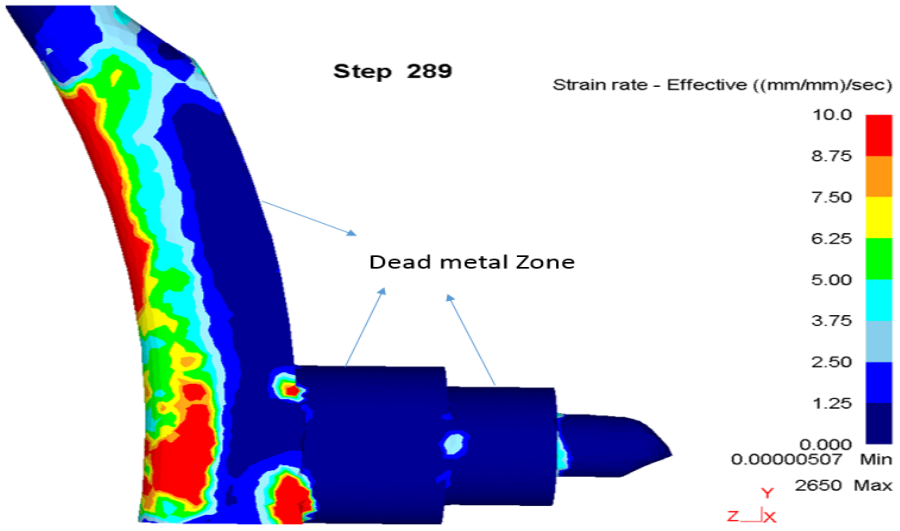

Figure 39. Strain rate distribution.

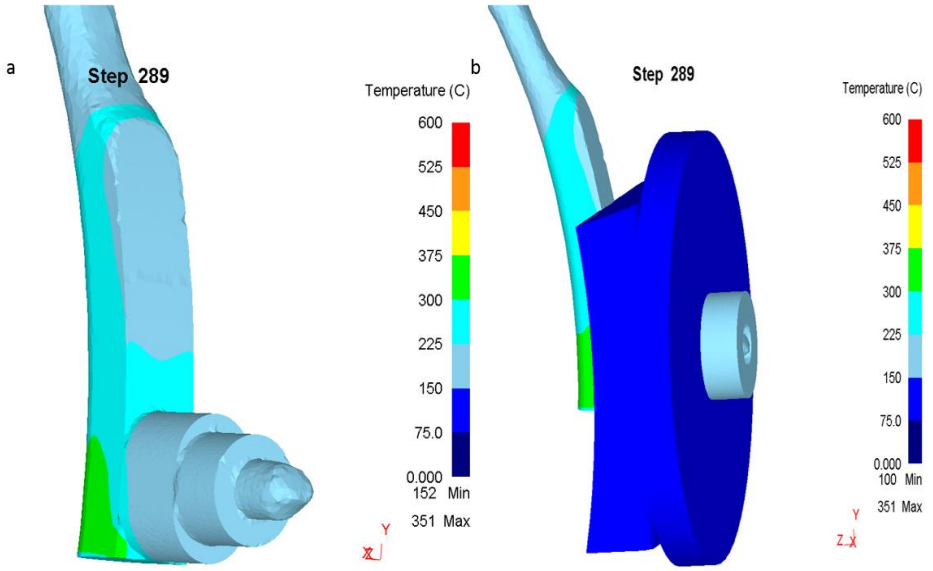

Figure 40. a) Temperature distribution of the work piece b) Temperature distribution of the deformation zone tooling.

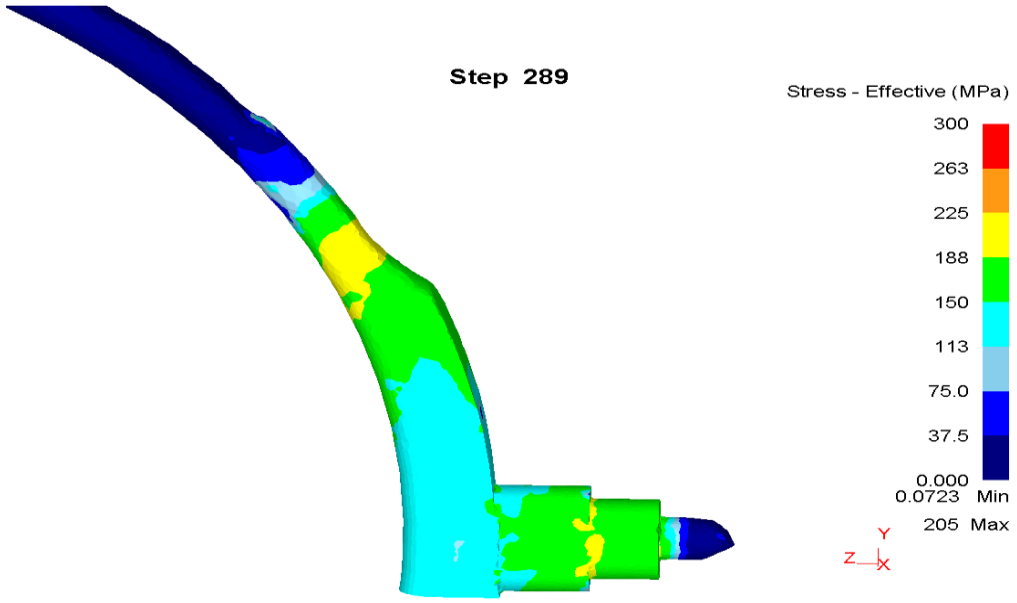

Figure 41. Effective stress distribution in the deformed AZ91 alloy during CRE.

3.2 Model 2

Figure 42 shows the extrudate of the model 2, the only difference between model 1 and 2 is workpiece temperature, in model 1 workpiece was at 350° C and in model 2 workpiece was kept at room temperature.

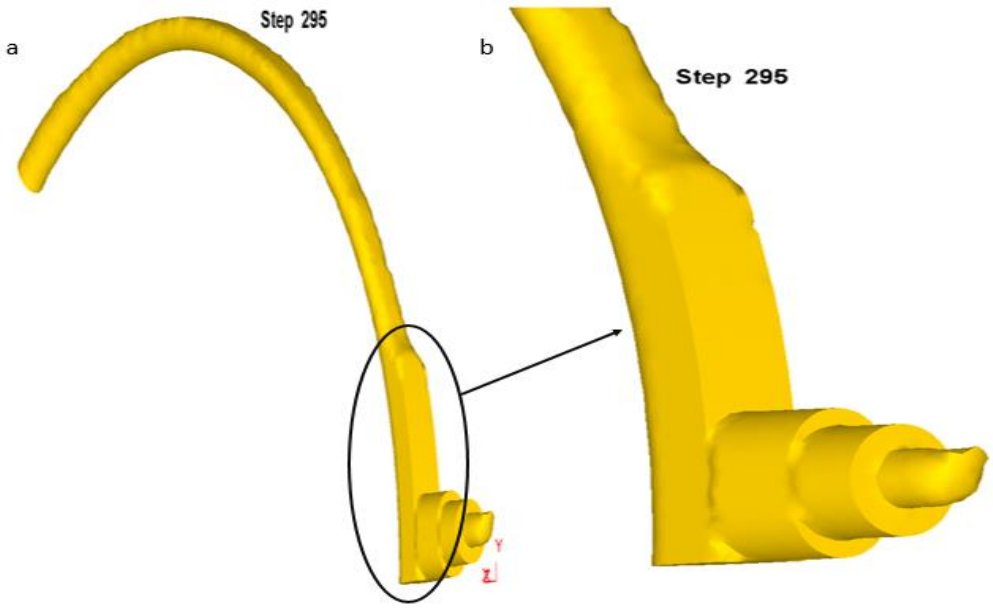

Figure 42. a) Model 2 Extruded profile. b) Buildup formation.

Figure 44a shows that the temperature rise in the workpiece is only due to plastic deformation and friction between tools and workpiece, since the workpiece was at room temperature at the beginning of the process temperature in the deformation zone of model 2 is less than that of model 1 shown in Figure 44b, which initiates plugging and causes the buildup formation. But length of the buildup zone is less in model 2 as shown in Figure 43, because the material has lower temperature at the buildup region in model 2, hence the material is not soft enough to allow for the buildup.

Observation of the Figure 45a and 47a allows making a statement that it is clear that there is no deformation in the buildup region in model 2 as the material is not soft enough and the heat generated by the plastic deformation is transferred to seal plate, which because of the lower temperature makes the material harder. But the material in the buildup zone moves as a rigid body when compared to the model 1 where there is a dead metal zone as shown in Figure 46.

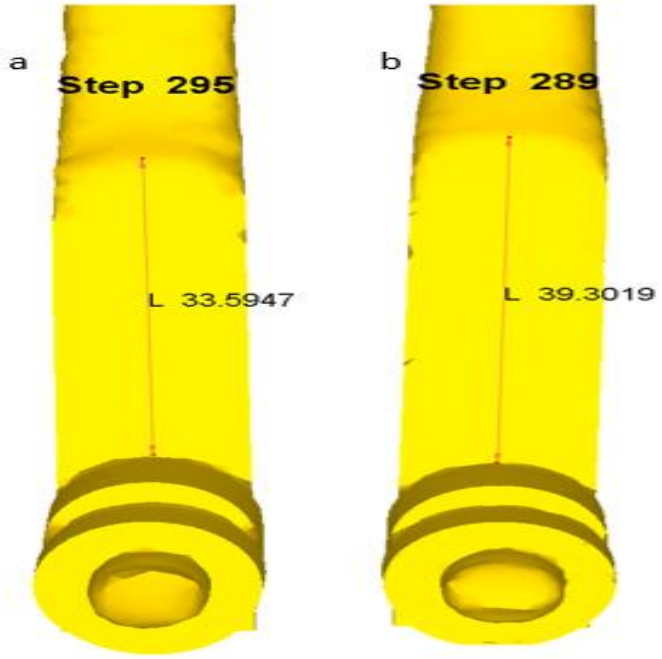

Figure 43. a) Length of the buildup in model 2 b) Length of buildup in model 1.

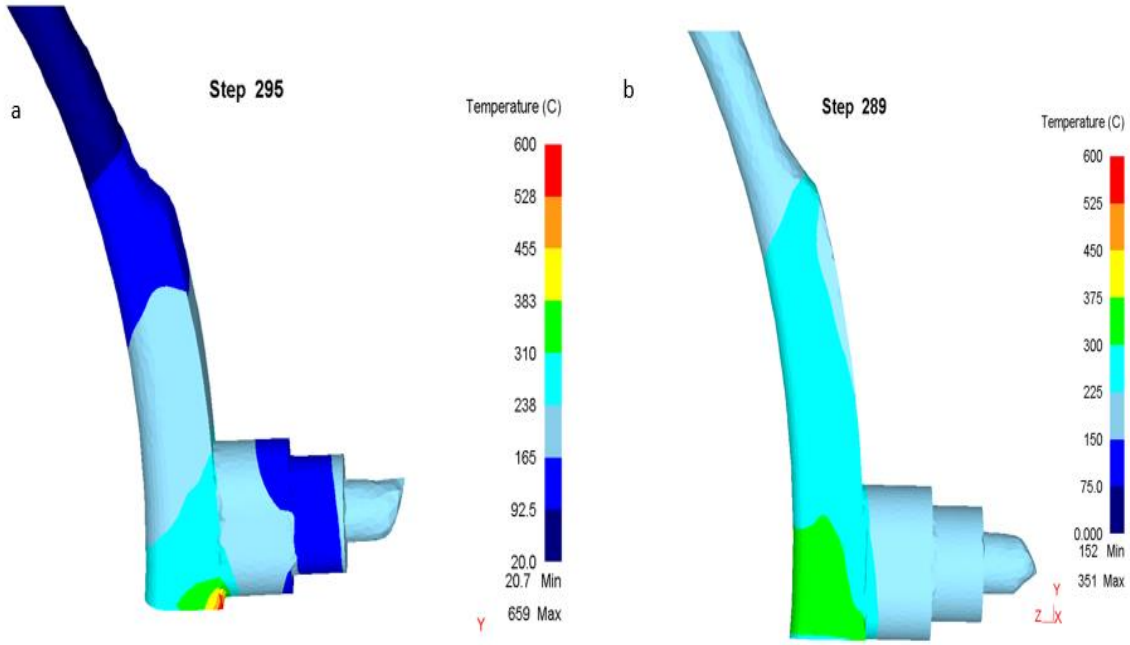

Figure 44. a) Temperature distribution in model 2 b) Temperature distribution in model 1.

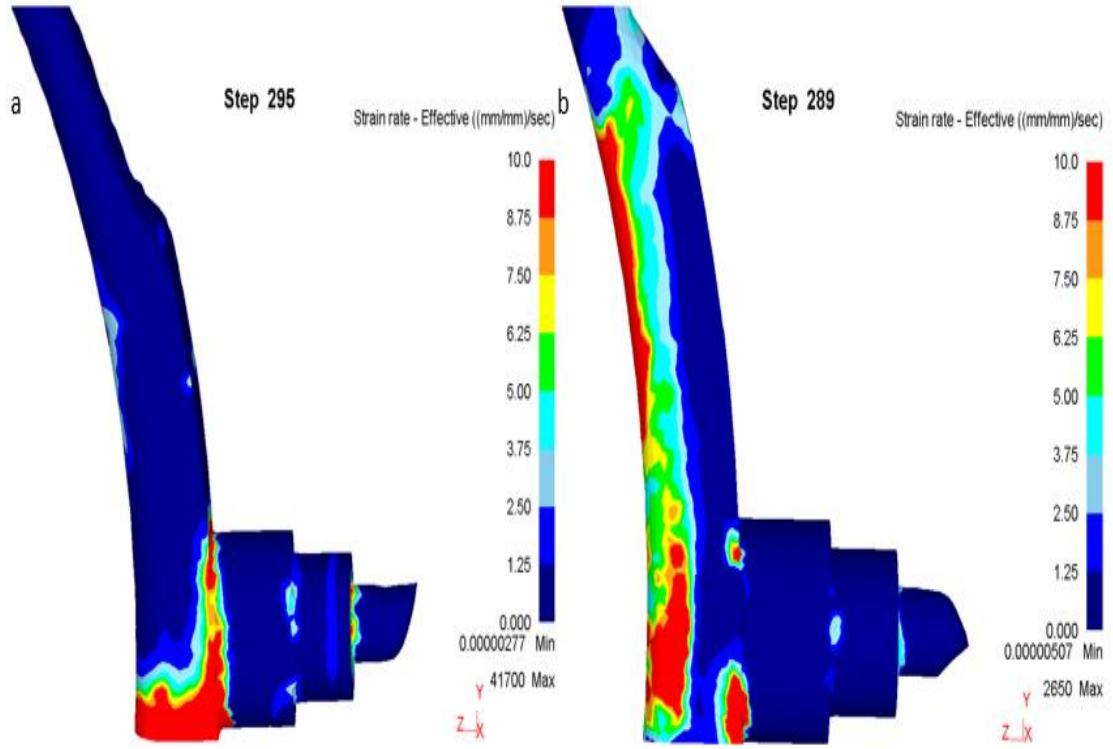

Figure 45. a) Strain rate distribution in model 2 b) Strain rate distribution in model 1.

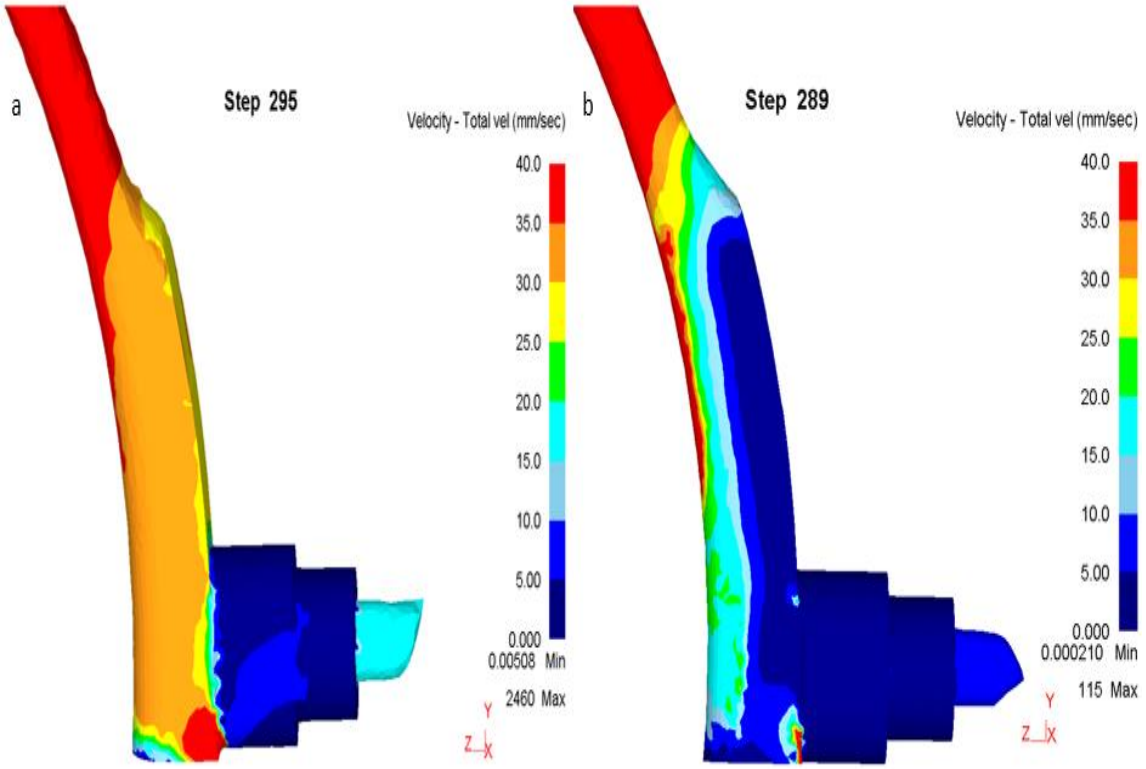

Figure 46. a) Velocity distribution in model 2 b) Velocity distribution in model 1.

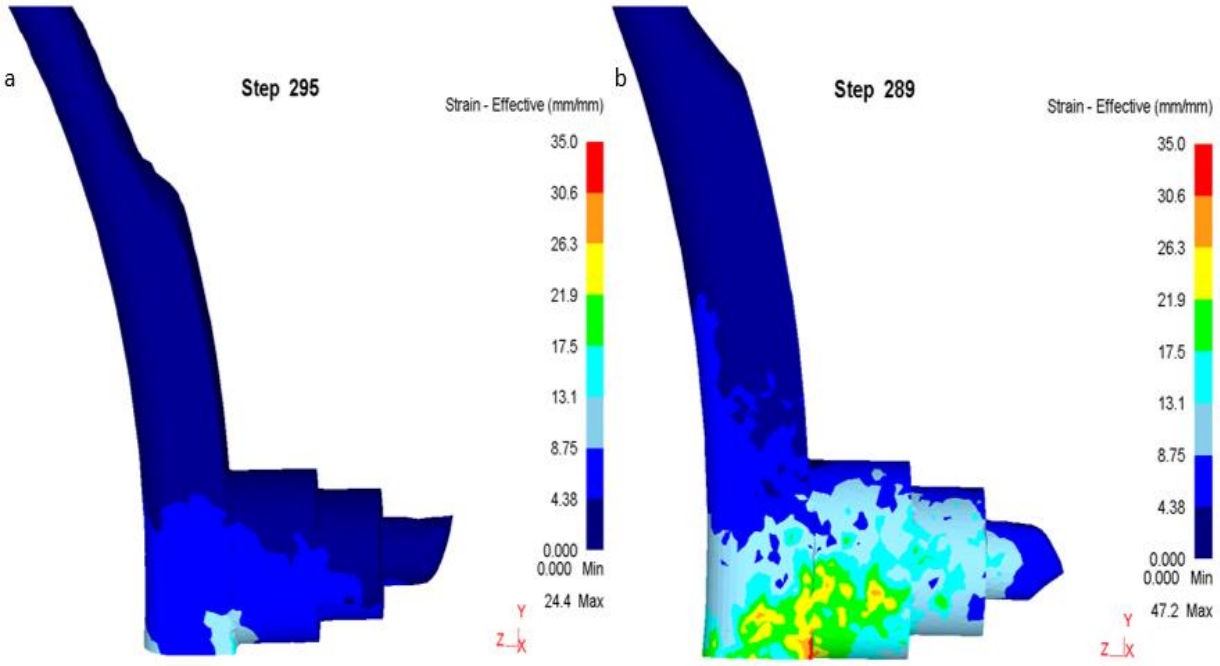

Figure 47. a) Strain distribution in model 2 b) Strain distribution in model 1.

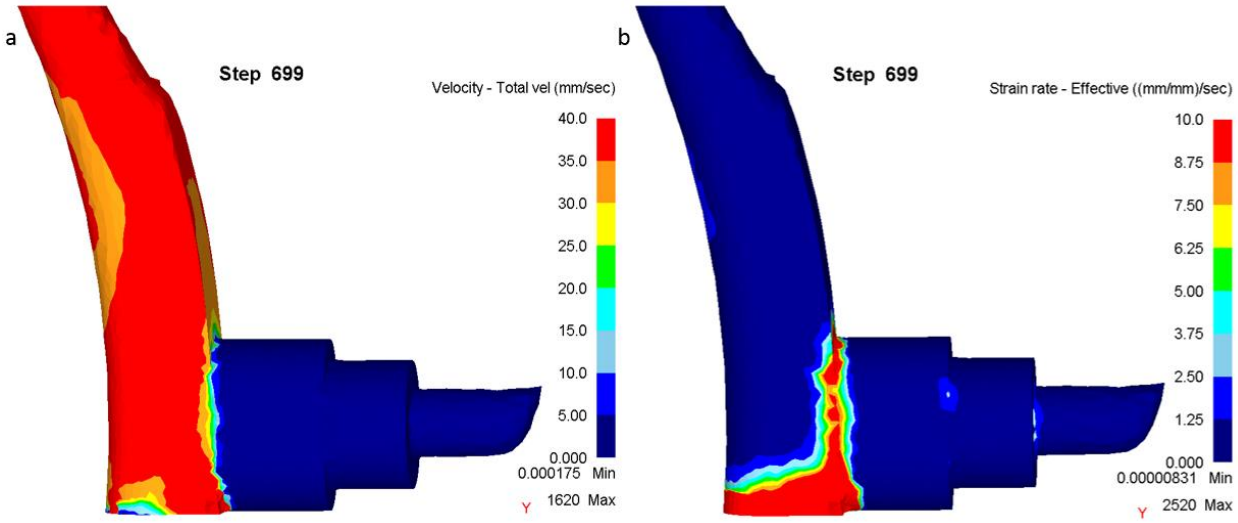

Figure 48. a) Velocity distribution of model 2 b) Strain rate distribution of model 2 on further running the model.

3.3 Model 3

Figure 49 shows the extruded profile of model 3, in which the workpiece is kept at room temperature, and the instead of 8mm diameter rod 9 mm diameter rod was extruded. The friction condition was changed, and the temperature of the tooling and deformation zone was changed as shown in Table 2. As one can see from the Figure 49 there is no buildup zone, but instead of that there is a small amount of metal fold (surface irregularities that appear as linear defects caused by folding over of hot metals at the surface) present as shown in Figure 50. This phenomenon could lead to defects due to oxide penetration.

As the metal is started to be extruded there will be some resistance to the metal flow by the die depending upon the extrusion ratio, which will make some of the metal to be squeezed out as shown in Figure 51, which is heated by the feeder plate as the metal comes in to contact with the feed plate hence it becomes softer and causes a whirl flow of workpiece material. As shown in Figure 52 there are dead metal zone along the edges of the O-ring and die, and there is a rigid body

flow at the center of the deformation zone. Figure 54 shows that maximum force acting in the region of upsetting.

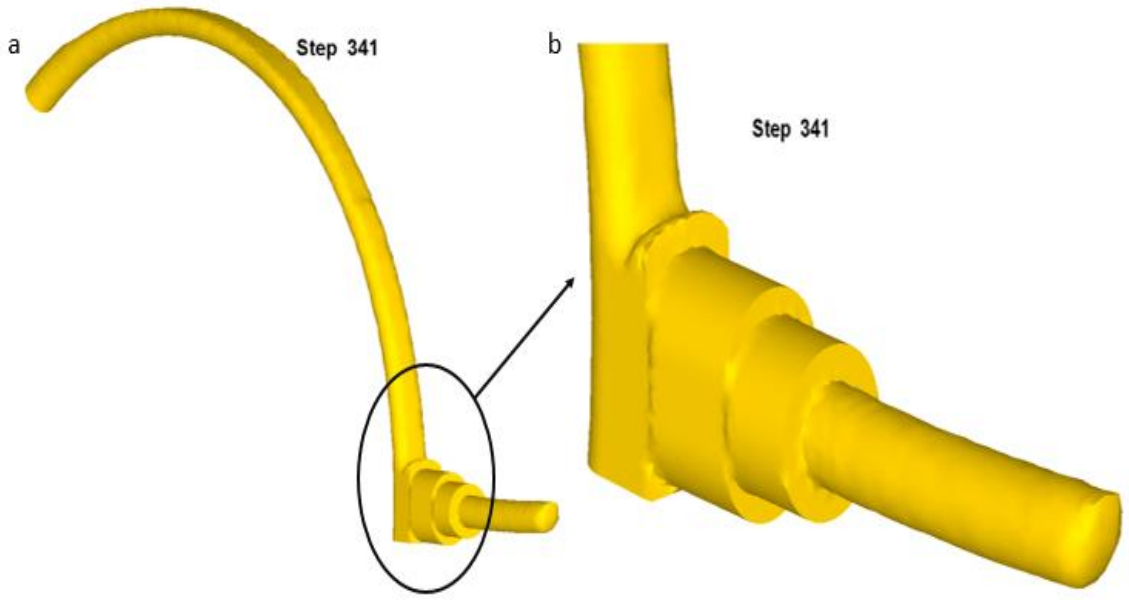

Figure 49. a) Model 3 extruded profile b) Deformation zone of the extruded profile.

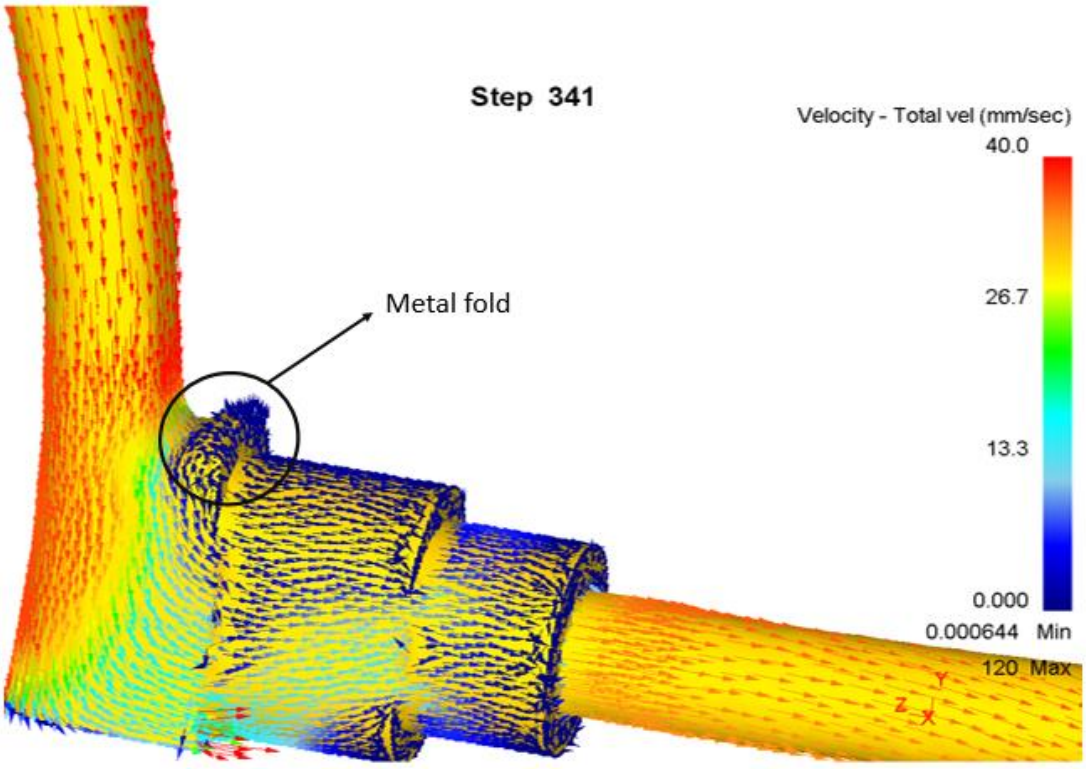

Figure 50. Velocity distribution with clearly shown metal folding.

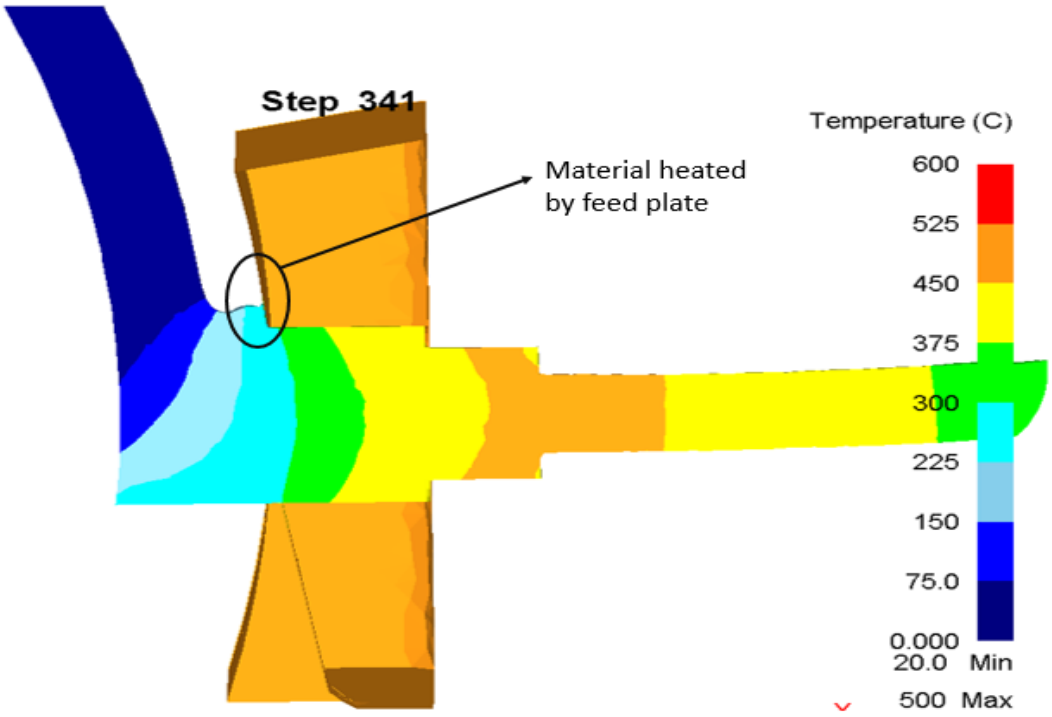

Figure 51. Temperature distribution in sectioned view.

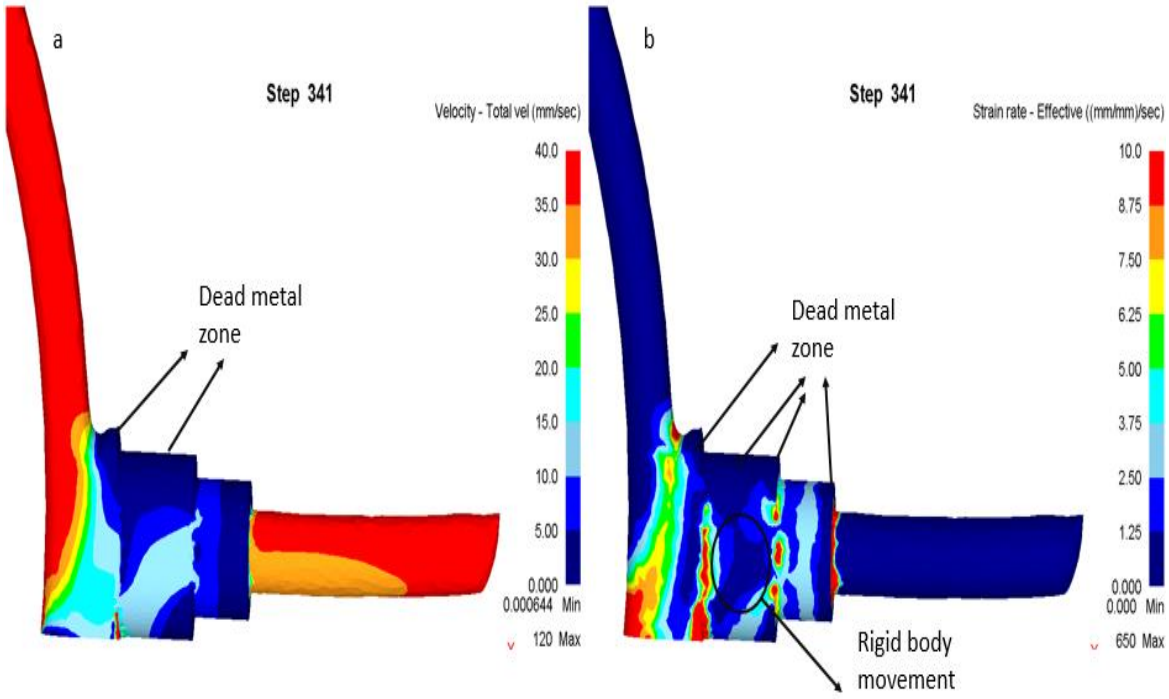

Figure 52. a) Velocity distribution of model 3. b) Strain rate distribution of model 3.

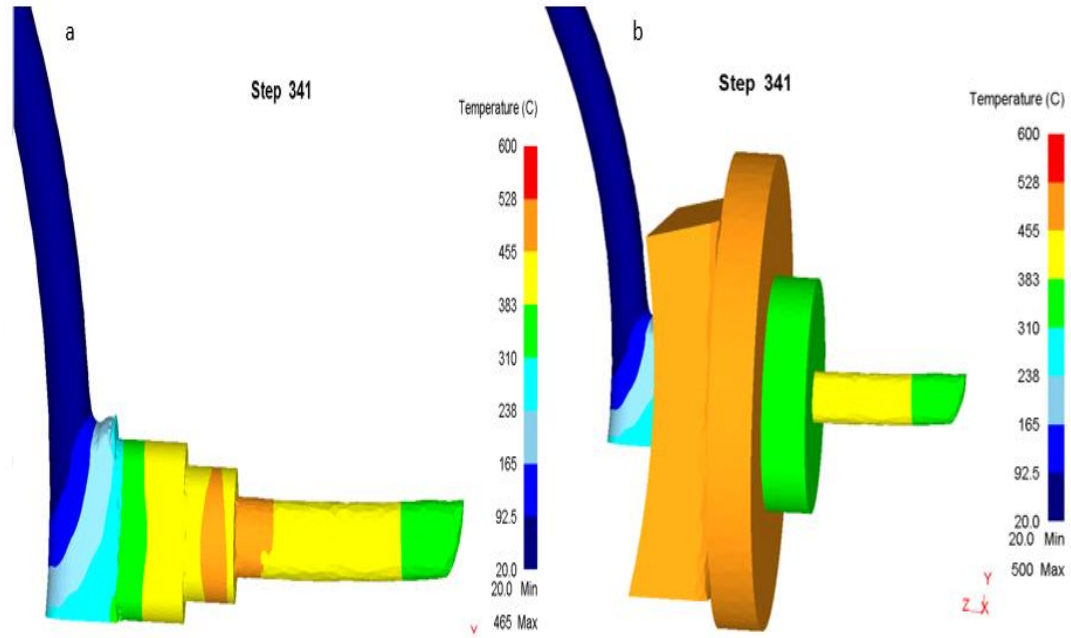

Figure 53. a) Temperature distribution of model 3. b) Deformation zone temperature of model 3.

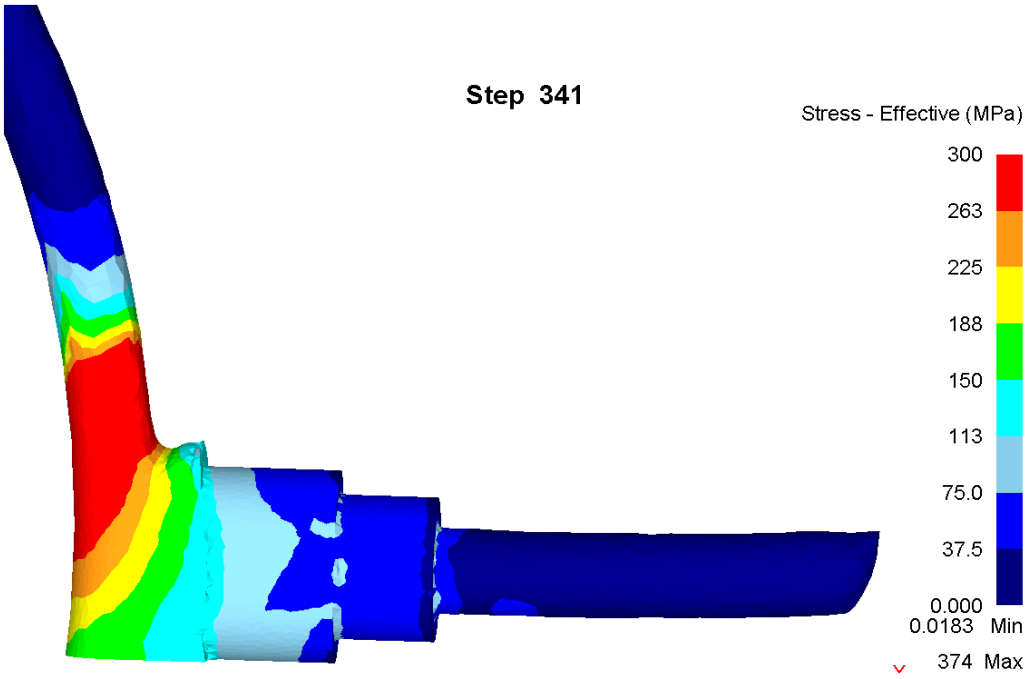

Figure 54. Stress distribution of model 3.

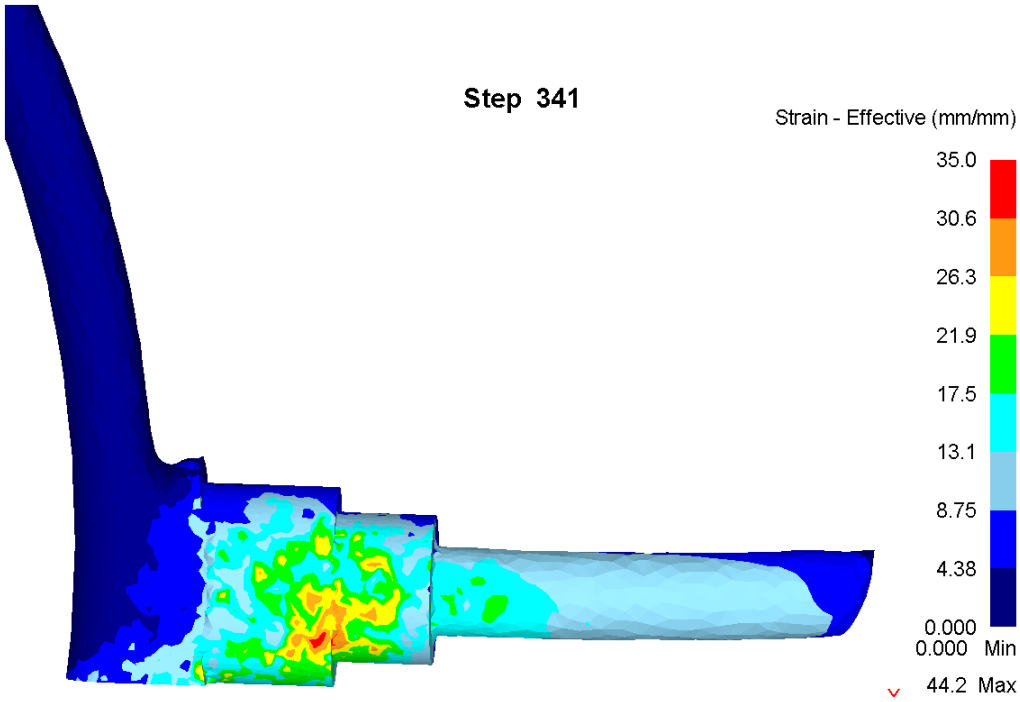

Figure 55. Strain distribution of model 3.

3.4 Model 4

Figure 56 shows the extrudate of model 4, the only difference between model 3 and 4 is that the extrusion ratio. Model 4 has higher extrusion ratio than model 3 with a value of 2. As the result of higher extrusion ratio the back pressure or the resistance by the die to the metal flow is stronger. Hence the metal folding as shown in Figure 57 and 58 is more predominant in model 4 than in model 3. If we compare the models 3 and 4 directly for temperature profile as shown in Figures 51 and 59, for velocity and strain rate profile as shown in Figures 52 and 60, for stress distribution as shown in Figures 54 and 62 and Figures 55 and 63 for strain profile we could see that both the models have same pattern but the only difference is magnitude.

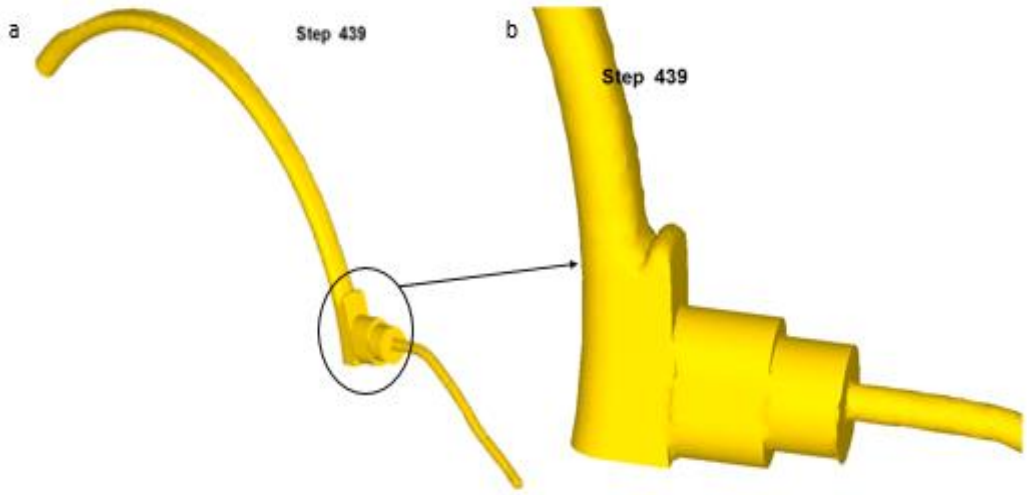

Figure 56. a) Model 4 extruded profile b) Deformation zone of the extruded profile.

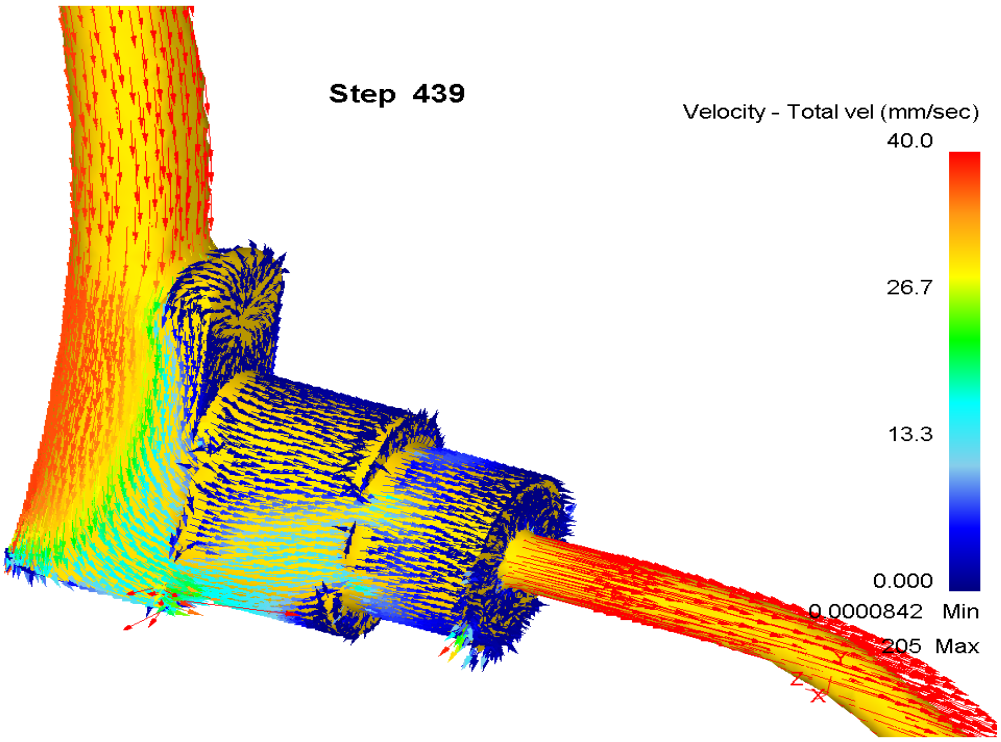

Figure 57. Velocity distribution with clearly shown Metal fold.

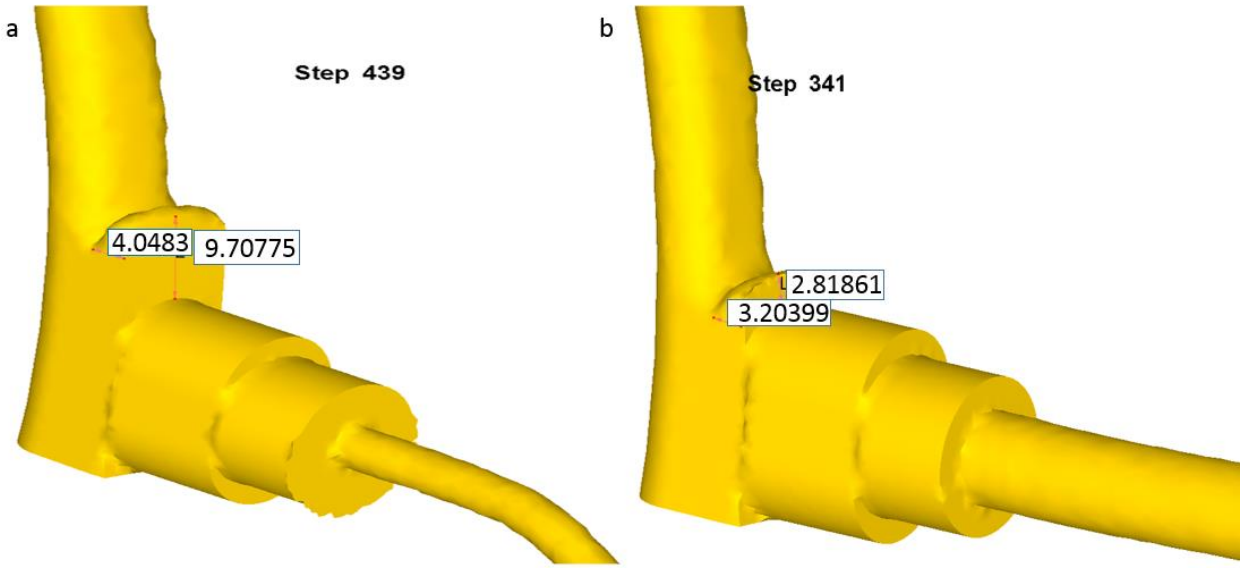

Figure 58. a) Buildup length of model 4 b) Buildup length of model 3.

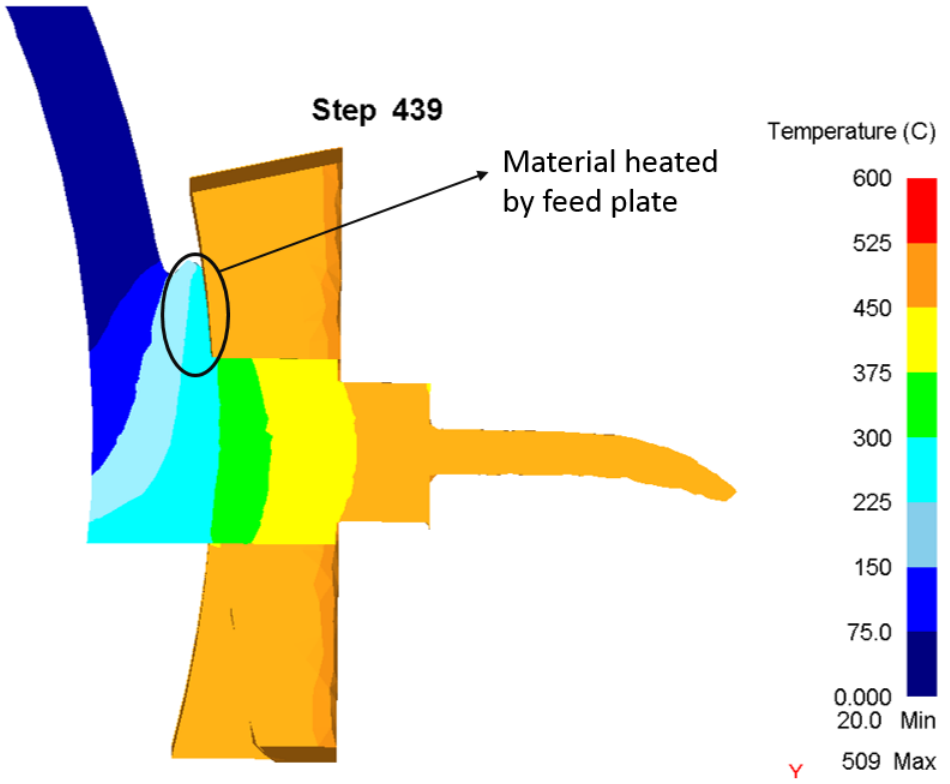

Figure 59. Temperature distribution of the extruded profile.

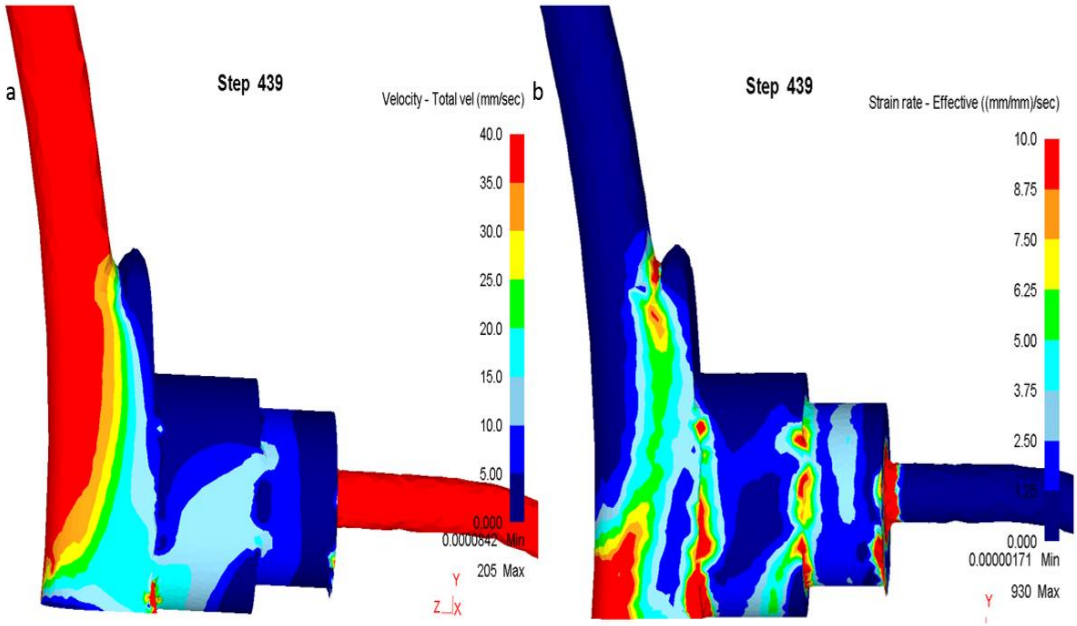

Figure 60. a) Velocity distribution of model 4 b) Strain rate distribution of model 4.

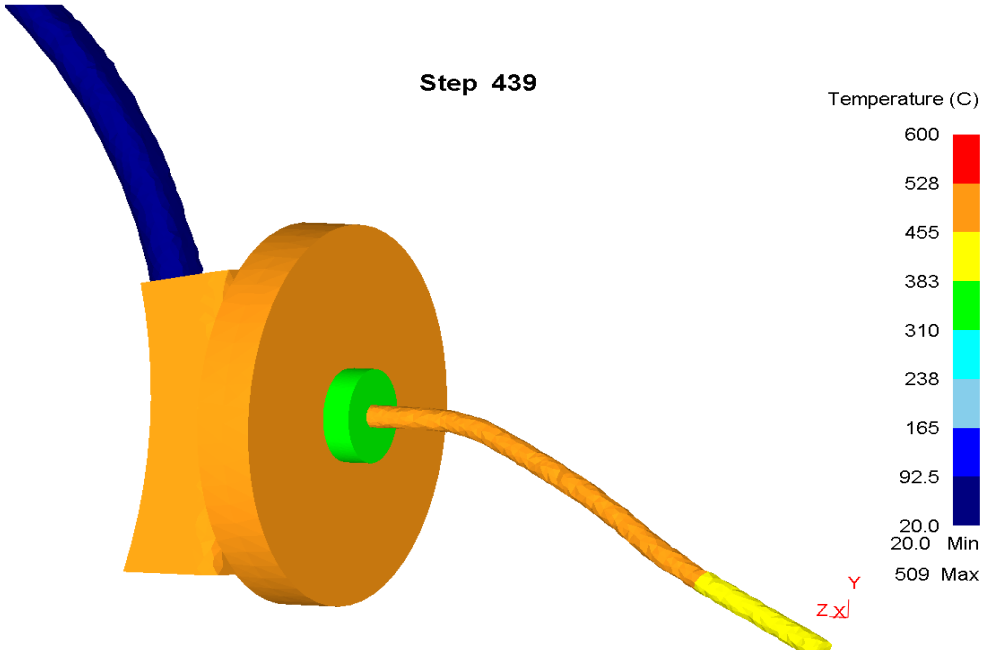

Figure 61. Deformation zone temperature.

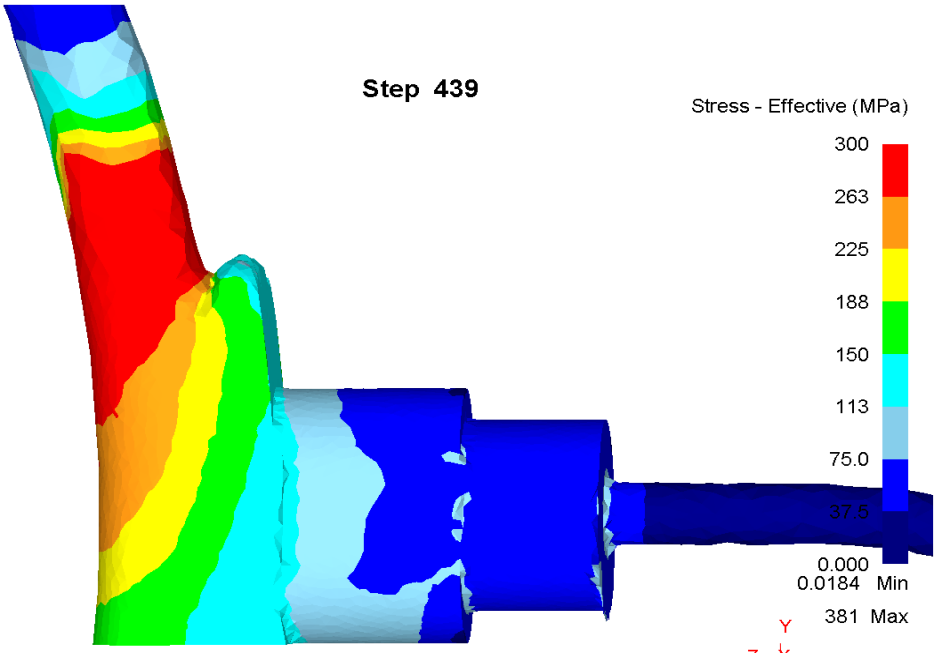

Figure 62. Stress distribution of model 4.

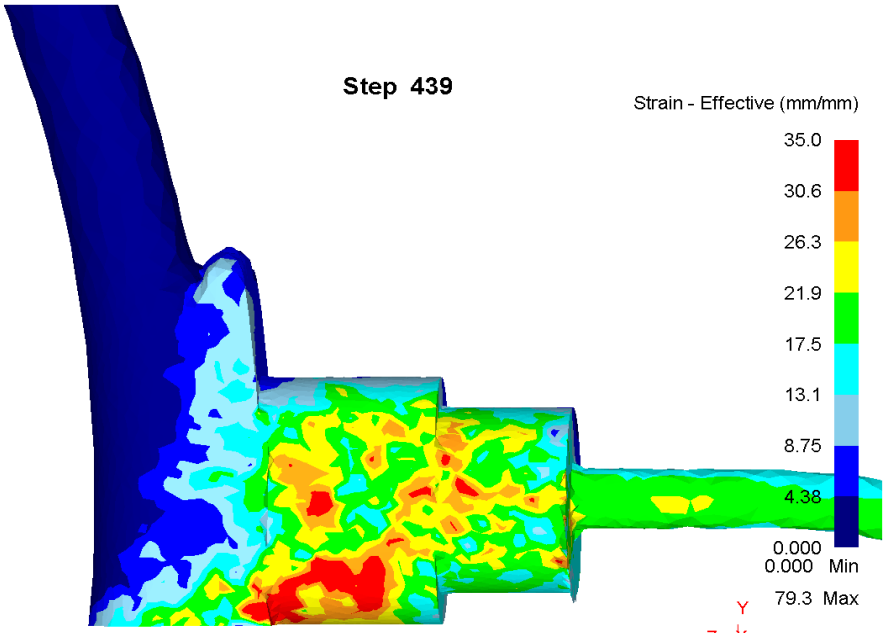

Figure 63. Strain distribution of model 4.

4 DISCUSSION

As one could see from Table 2 the major difference between the model 1 and model 2 was the workpiece temperature, while the other process parameters were kept the same. From Figure 44 one can see that there is a difference in temperature distribution in the buildup region and deformation zone for model 1 and model 2, which causes the rigid body movement in the deformation zone in case of model 2. There is no movement in the deformation zone in model 1 as shown in Figure 45b and 46b, due to the higher temperature in the buildup region and lower temperature in the deformation zone of model 1. It can be seen if we observe the temperature distributions of buildup region and deformation zone of model 2 as shown in Figure 44a and b. The temperature distribution in model 1 makes the material in the deformation zone harder and material in the buildup region softer. Hence the material plugs at the die exist and starts to buildup in the other end. This difference in temperature distribution is mainly caused by the difference in

workpiece temperature as it was assumed for model 1 and model 2. The plugging of workpiece in the deformation zone will eventually happen in model 2 as shown in Figure 48, but it would take much longer time than in model 1. Hence form the results of both models it is clear that workpiece temperature does not have a huge impact on the buildup formation and plugging, however it would influence the time of its formation. Deformation zone temperature, wheel temperature and shoe temperature are the parameters which have a huge impact on the buildup formation.

Figures 44a and b shows the temperature of the buildup region in both model 1 and 2 are at a temperature range of 200-300°C (approx.), The flow stress data as shown in Figure 36b is very sensitive in the range of 20 -300°C, in the current model there is no data point 20 to 350°C. So to better understand the buildup formation more flow stress data in range of 20-300°C is needed.

There is a difference in temperature distribution between model 1, 2 and model 3 if one compare it directly as shown in Figure 44 and 51, which cause the different metal flow in model 1, 2 and model 3 as shown in Figure 38b and 50. Hence the metal folding phenomenon was not found in model 1 and model 2. In model 3, however this whirl movement of workpiece as shown in Figure 50 which makes the workpiece material to flow into the cavity in such a manner that initial surface of the workpiece is folded on the top of itself entrapping the air in the cavity causing a defect. Entrapped air will oxidize the surface preventing it from joining.

As shown in Table 2 the only difference between model 3 and model 4 is extrusion ratio, while other parameters were kept the same. As one could see from Figure 56-58 the metal folding phenomenon is more dominant in model 4 when compared with model 3. This is mainly caused by two things, one factor is the extrusion ratio as shown in Table 2 and the other is heating of workpiece material by the heat transfer occurring between feeder plate and workpiece material, making it softer as shown in Figure 59. If one directly compare Figure 51 and 59, it will show the

difference in amount of workpiece material in contact with feeder plate and heated by it. This difference in the amount of workpiece material in contact with the feeder plate in model 3 and 4 is mainly due to the reason that model 4 has higher extrusion ratio as shown in Table 2. Due to the high extrusion ratio in model 4 the resistance to metal flow is higher in model 4, hence workpiece material are pushed in to the cavity between the groove and the shoe at higher velocity. These material are heated by the feeder plate, and makes it softer, which cause the whirl movement leading to metal folding.

In model 1 and 2 the input material is softer due to higher billet temperature, and heating by the rotating wheel. This high temperature input material when comes in contact with the deformation zone tooling and the shoe which are at lower temperature, large amount of heat is transferred from the input workpiece material to the deformation zone tooling and shoe. Which cools down the workpiece material making it harder. Since the material in the deformation zone is harder, more amount of force is required to push it through the die orifice, but the input material will not be able to apply this required force on the material which is in the deformation zone as it is softer. This is the reason the softer input material just buildup on the harder material in deformation zone. As the result of this plugging phenomenon happens creating no output. In model 3 and 4 the input material was harder and the material in the deformation zone was heated by the deformation zone geometry making it softer. Hence there was no plugging or buildup formation in model 3 and 4 as the material in the deformation zone was softer, it was easily pushed by the harder incoming feed material. One could also see folds occurring in model 3 and 4, which can be avoided by better deformation zone design.

This numerical model could be a perfect tool for comparing the experimental results and understand the actual process to the core and improve it. As this model can be updated with the

real life parameters such us friction, temperature, wheel velocity, extrusion ratio, material model which will helps as to determine the strain, strain rate and stress at any point of time. This is very difficult, or even impossible to achieve in the actual physical experiment not mentioning its cost.

5 CONCLUSION

The FEM modeling has provided information on the basic metal flow in early stages of the CRE process. Based on the numerical simulation results the following conclusions are made:

- During filling stage it is important to maintain low temperature of the feed rod being pressed against the abutment and high temperature on the metal stream fed from the abutment into the die otherwise plugging of workpiece material will happen.
- Deformational and metal forming condition of Magnesium alloy formed in the CRE process seems to be well described by the DEFORM-3D – models and seems to be capable of predicting how processing in CRE is affected by the process parameters.

6 FUTURE WORK

Areas where an additional work is suggested in FEM simulation of the CRE process are as follows:

- Improving material model for wider range of temperature to make the FEM model more accurate.
- Inputting the accurate boundary condition like temperature of the tooling, friction etc., of the real-world process into the FEM model.
- Performing detailed parametric studies which includes changing wheel velocity, extrusion ratio, deformation zone temperature, deformation zone geometry, friction condition, billet temperature etc.,

- Comparing FEM results with the experimental data to validate the model.
- Detailed study of metal flow for different deformation zone geometry.
- Identifying the select scenarios of intersect to verify with the industrial extrusion press and performing the experimental extrusion runs.
- Determination of optimum process condition to obtain desired grain structure.

REFERENCE

[1] Mordike B.L, Ebert T, Magnesium Properties Application Potential, Materials Science and Engineering, Vol. A302; 2001; pp. 37–45.

[2] Hai Hao, Casting technology and Quality Improvement of Magnesium alloys, Special Issues on Magnesium Alloys, 1st ed.: InTech, 2011.

[3] Soomro M.W, Neitzert T.R, Effects of pre-process and post-process parameters on formability of Magnesium alloys, Journal of Achievements in Materials and Manufacturing Engineering, vol. 55; 2012; pp. 799-809.

[4] ASM Specialty Handbook: Magnesium and magnesium alloys, 1st ed.: ASM International, 1999.

[5] Raghunath B.K, Raghukandan K, Karthikeyan R, Palanikumar K, Pillai U.T.S, Ashok Gandhi R, Flow stress modeling of AZ91 Magnesium alloy alloys at elevated temperature, Journal of Alloys and Compounds, Vol.509 ;2011;pp. 4992-4998.

[6] Mamoru Mabuchi, Kohei Kubota, Kenji Higashi, New Recycling Process by Extrusion for Machined Chips of AZ91 Magnesium and Mechanical Properties of Extruded Bars, Materials Transactions, JIM, vol.36, no. 10(1995), pp.1249 - 1254.

[7] Hiroyuki Watanabe, Toshiji Mukai, Koichi Ishikawa and Kenji Higashi, High-Strain Rate Superplasticity in an AZ91 Magnesium Alloy Processed by Ingot Metallurgy Route, Materials Transactions, Vol. 43, No. 1; 2002; pp. 78 to 80.

[8] Ravi Kumar N.V, Blandin J.J, Desrayaud C, Montheillet F, Sue´ry M, Grain refinement in AZ91 Magnesium alloy during thermomechanical processing, Materials and Engineering Vol. A359; 2003; pp. 150-157

[9] Liu G, Zhou J, Duszczyk J, FE analysis of metal flow and weld seam formation in a porthole die during the extrusion of a Magnesium alloy into a square tube and the effect of ram speed on weld strength, journal of materials processing technology, vol. 200; 2008; pp. 185–198.

[10] Grorge E. Dieter, Mechanical Metallurgy, 3rd ed.: McGaw-Hill, 1986.

[11] Bauser.M, Sauer.G, Siegert.K, Extrusion, 2nd ed.: ASM International, 2006; pp.59-126.

[12] Henry S. Valberg, Applied Metal Forming Including FEM Analysis, 1st ed.: Cambridge University Press, 2010; pp. 219-241.

[13] Clifford Etherington, Harold Kieth Slater, The Extrusion of Aluminium and its Alloys by CONFORM Process, Proceedings of the third international aluminum extrusion technology seminar, 1984.

[14] Laue.K, Stenger.H, Extrusion, 2nd ed.: American Society for Metals, 1976.

[15] Junying Yang, Baoyun Song, Haishi Ning, Rong Fu, "Microstructure of AZ31 Magnesium Alloy Produced by the CONFORM Process under Different Extrusion Wheel Velocities" Advanced Materials Research, vol. 189-193; 2011; pp. 2609-2612.

[16] Cho J.R, Jeong H.S, "Parametric investigation on the curling phenomenon in CONFORM process by three-dimensional finite element analysis" Journal of Materials Processing Technology vol. 110; 2001; pp. 53-60.

[17] Cho J.R, Jeong H.S, CONFORM process: surface separation, curling and process characteristics to wheel diameter, Journal of Materials Processing Technology vol. 136; 2003; pp. 217-226.

[18] Parkinson R.D, The Technical Development of a New Extrusion Company Solely Using Conform Machine, Fourth International Aluminum Extrusion Technology Seminar, 1988.

[19] Monika Mitka, Maciej Gawlik, Mariusz Bigaj, Wojciech Szymanski, Continuous Rotary Extrusion (CRE) of Flat Sections from 6063 Alloy, Key Engineering Material, vol. 641; 2015; pp. 183-189.

[20] Molyneux R.H, Present Capability and Future Potential of the CONFORM/CONKLAD Universal Machine, Fourth International Aluminum Extrusion Technology Seminar, 1988.

[21] Kim Y.H et al, A study on optimal design for CONFORM process" Journal of Materials Processing Technology, vol. 80–81; 1998; pp. 671–675.

[22] Junying Yang et al, Microstructure of AZ31 Magnesium Alloy Produced by the Conform Process under Different Extrusion Wheel Velocities, Advanced Materials Research, vol. 189-193; 2011; pp. 2609-2612.

[23] Monika Mitka, Wojciech Z.Misiolek, Marzena Lech- Grega, Maciej Gawlik, Mariusz Bigaj, Wojciech Szymanski: Continuous rotary extrusion of Magnesium alloy AZ91, Continuous Rotary Extrusion of Magnesium Alloys within the Institute for Non-Ferrous Metals, Light Metal Division, project report 7296/2914.

[24] Zener C, Hollomon J.H, Effect of Strain Rate upon Plastic Flow of Steel, Journal of applied physics, 1943

[25] Takuda .H, Fujimoto .H, Hatta .N, Modelling on flow stress of Mg-Al-Zn alloys at elevated temperature, Journal of Material Processing Technology, vol. 80-81; 1998; pp. 513-516.

[26] Sheng. Z.Q, Shivpuri .R, Modeling flow stress of magnesium alloys at elevated temperature, Material Science and Engineering, vol. A419; 2006; pp. 202-208.

[27] Sellars C.M, Tegart, Mem. Sci. Rev. Metall, vol. 63; 1996; pp. 731-746.

[28] Pietzka D, Becker D, Ben Khalifa N, Donati L, Tomesani L, Tekkaya A.E, Extrusion Benckmark 2009 – Benchmark Experiments: Study on Material flow, Die Deflection and Profile Distortion, Advances in Extrusion Technology and Simulation, 2009.

[29] Asadi P, Mahdavinejad R.A, Tutunchilar S, Simulation and experimental investigation of FSP of AZ91 magnesium alloy, Materials science and Engineering vol. A528; 2011; pp. 6469-6477.

[30] Chamanfar A, Jahazi M, Gholipour J, Wanjara J, Yue S, Evolution of flow stress and microstructure during isothermal compression of Waspaloy, Material Science & Engineering, vol. A615; 2014; pp. 497-510.

[31] Private conversation with Professor Henry S. Valberg, Norwegian University of Science and Technology.

VITA

Nijenthan Rajendran was born in March 21, 1992 in Madurai city, TN, India to his parents M. Rajendran PhD., and R.A. Sasikala MA. He did his schooling in the same city. He began his university career in PSG College of Technology in Coimbatore, TN, India as a sandwich Mechanical Engineer. During that time he worked in Ford India PVT Chennai, India as an intern for 2 months. In his undergrad times he was an active member of American Society of Mechanical Engineering ASME, where he has organized many events. As his final year project he worked in collaboration with the company Sree Durga Metals and Alloys in Coimbatore, India in implementing Lean in their company. After completing his undergraduate in 2014, he joined in Lehigh University as a master student in Mechanical engineering and mechanics department.